ACKNOWLEDGEMENTS

First and foremost I am extremely thankful to the most merciful Allah Almighty who grants me the strength and power to finish my work in time and the Holy Prophet Muhammad (PBUH) who is the positive code of life for all human beings. I wish to express my sincere gratefulness to my supervisor, Dr. Syed Tahir Raza Rizvi, who has the substance of a genius: he competently guided and encouraged me to be professional and do the right thing even when the road got tough. Without his persistent help, the goal of this project would not have been performed. I would also like to thank Dr. Kashif Ali for their research-based support in my study and also like to thank all my teachers and friends. Finally, I wish to acknowledge the presence of support and the great love of my family. They held me proceeding and this work would not have been possible without their prayers.

Syed Oan Abbas Bukhari

CIIT/SP20-RMT-039/LHR

Abstract

Numerical and Exact Solutions for Various Nonlinear Evolution Equations

A soliton is a particular type of solitary wave, that is retrieved as a result of integrable NLPDE. There are different type of solutions like analytic and approximate solutions exist. An exact solution is a symbolic representation of a value which solves a given equation exactly, while a numerical solution is numerical representation of a value which solves a given equation exactly or approximately. Numerical solutions are very usefull when we are unable to retrieve analytic solution. It is also used for comparison with analytic solutions. A lot of analytic and numerical methods exists in literature to solve the NLPDEs such as Bernouli's equation approach, extended tanh method, modified simple equation method and RK methods etc.
In this work, our purpose is to attain bell-type, kink and anti kink type, singular solitons and power series solutions for various forms of NLEEs. We'll also obtain Weierstrass elliptic functions, Jacobi elliptic functions in terms of hyperbolic, trigonometric and rational functions. In this thesis, we'll study various forms of NLEEs to attained these types of solutions with the help of various method like sine-cosine method (SCM), csch method, tan-cot method, sub-ode technique and residual power series method (RPSM). We will also compare our exact solutions with numerical solutions and then represent these solutions graphically.

Key words: Nonlinear evolution equations.

TABLE OF CONTENTS

LIST OF FIGURES

Chapter 1

Introduction

1.1 Soliton

A soliton is a particular type of solitary wave, that is retrieved as a result of NLPDE. The important property of a soliton is that it conserve its shape and speed during propagation as well as when collides with other solitons. Solitons can be formed in a mixture of materials and are used for various purposes. In a few substances, solitons may take electrical charges, when these charge solitons travel over numerous polymer chains, chains tends to curves. One day, this application can be used in artificial muscles. Solitons are also used in communications, since they can transfer a large amount of data over huge distances along without distortion in signals. The wide applicability of the solitons implies soliton phenomena that are common in various fields of physics. Solitons play an important role in almost all branches of physics, such as nonlinear optics, particle physics, nuclear physics, plasma physics, biophysics, astrophysics, hydrodynamics, low-temperature physics and condensed matter physics.

1.2 Types of solitons

Bell-type soliton Bell solitons are also called non-topological solitons. We find bell shape solutions of those nonlinear PDEs which having low frequency solitons solution. The solitons solutions of nonlinear KDV and NLSE equations have a bell shape and do not depend on amplitude and high frequency solution.

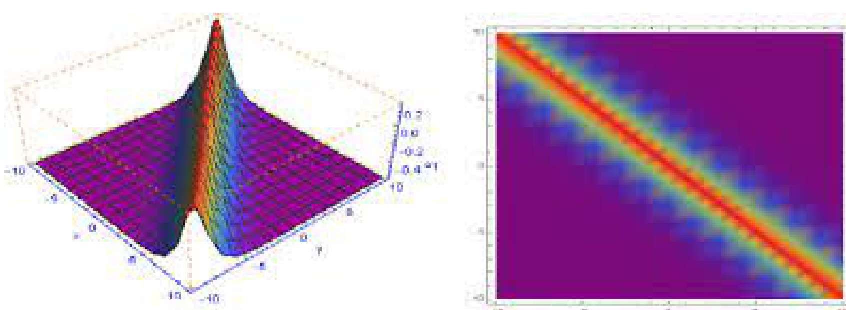

Figure 1.1: Bell type soliton.

Kink and Anti-kink type solitons are travelling wave solutions which ascend or descend from one phase to another. Kink and anti-kin soliton reaches a constant at infinity.

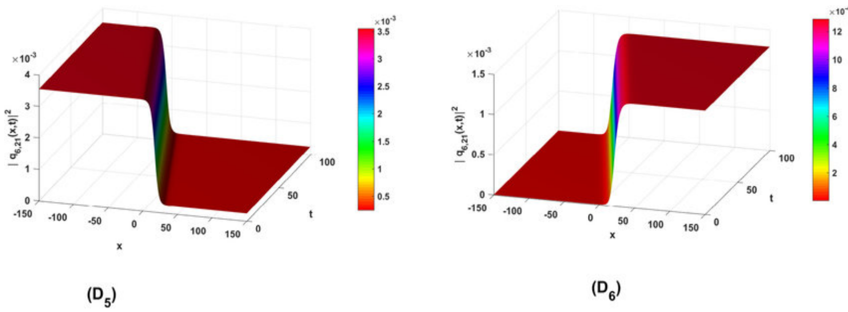

Figure 1.2: Kink and anti-kink type soliton.

Singular solitons The solutions having this form called Singular solitons.

$$\Phi(z,t) = \delta coth^{\alpha}(\eta), \quad \eta = \lambda(z - \nu t), \tag{1.2.1}$$

where δ, λ and ν denotes the amplitude, inverse width and velocity of soliton and $\alpha > 0$.

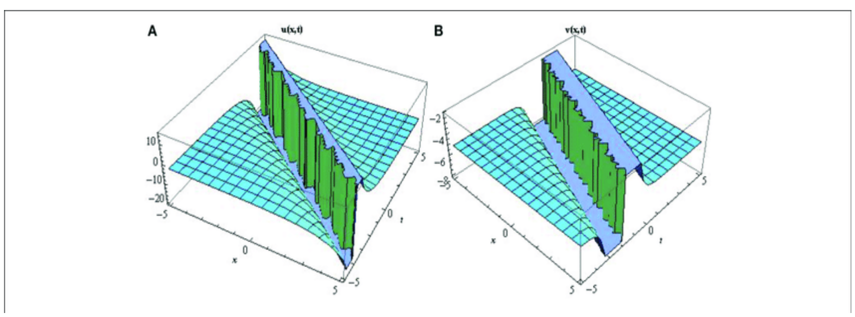

Figure 1.3: Singular soliton.

Bright solitons are the wave packets of light which arrange a specific energy and shape, without any change they have the ability of propagation over significant distances and it spread with a similar speed. In a particular water profundity range bright solitons can arise alongside dark solitons. These pulses keep their shapes and speed after their collision. The bright solitons are named as non-topological waves. The form of bright solitons is,

$$\Phi(z,t) = \delta sech^{\alpha}(\eta), \quad \eta = \lambda(z - \nu t), \tag{1.2.2}$$

where δ, λ and μ denotes the amplitude, inverse width and velocity of soliton and $\alpha > 0$.

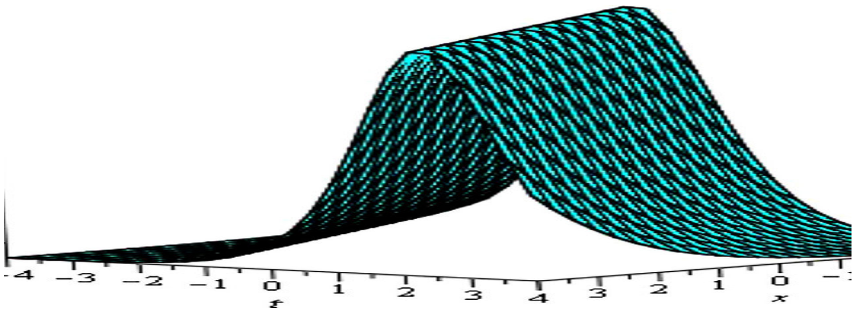

Figure 1.4: Bright soliton.

Dark solitons are the pules of haziness inside a continuous wave, having a particular shape and furthermore keep up their properties of spread. A contrast between the dark and the bright solitons is that alternately to a bright soliton the speed of a dark soliton relies on its amplitude. The dark solitons happens for the self-defocusing nonlinearities. Solitary wave form of the dark solitons is:,

$$\Phi(z,t) = \delta tanh^{\alpha}(\eta), \quad \eta = \lambda(z - \nu t). \tag{1.2.3}$$

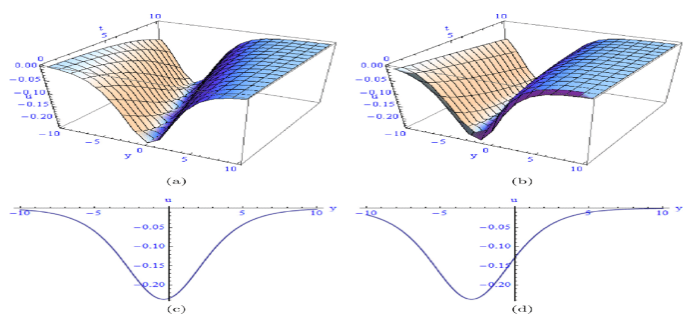

Figure 1.5: Dark soliton.

Peakons.

Highly peaked solitary wave solutions can also be read as peakons. These kind of waves are smooth except at a corner of its crest.

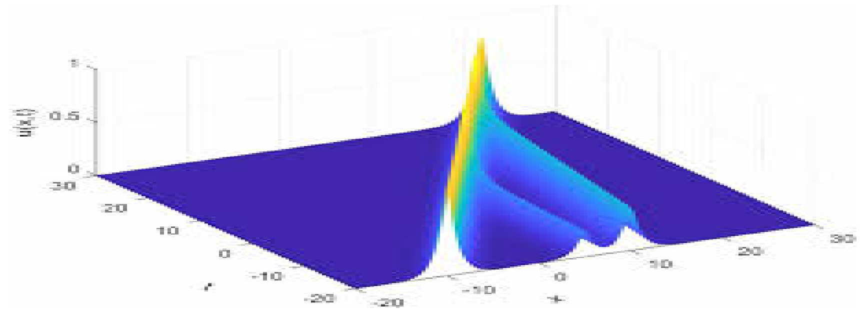

Figure 1.6: Peakons.

Cuspons.

When a solution exhibits cusps at their crests then we get another form of soliton which is called cuspons.

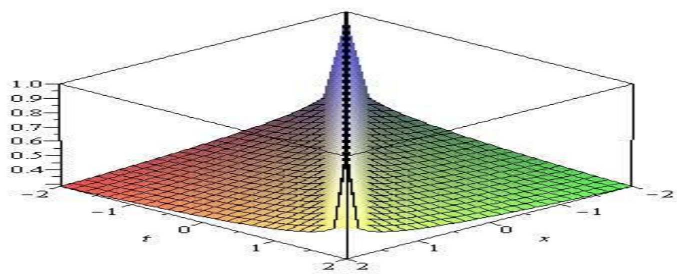

Figure 1.7: Cuspons.

Compactons.

A solitons with compact spatial support is known as compactons. Compactons has special characteristic that even two solitons collide with each other then they regain their shape and speed.

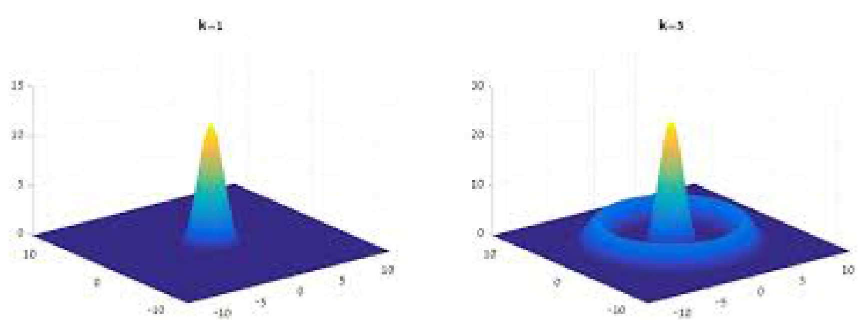

Figure 1.8: Compactons.

Periodic Solutions.

A travelling wave with cosine or sine function is known as periodic solution.

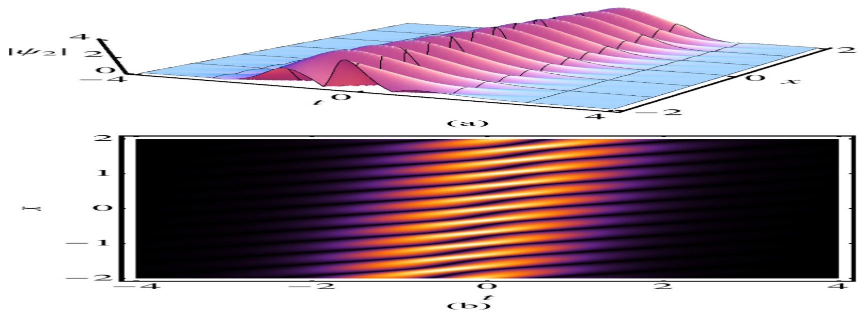

Figure 1.9: Periodic soliton solution.

1.3 Nonlinear evolution equation

The evolution equation have time derivative term, that is described as

$$g_t + a g_{xx} + b g_{xt} = 0 \tag{1.3.1}$$

NLEEs are very important in different field of sciences [1]. They have a lot of applications in various fields, especially in nonlinear science, nonlinear optics, mathematical physics, nonlinear mechanics, atmospheric science,, marine science, particle physics etc. NLEEs justify many environmental segments of nonlinear waves explained by equations and their solutions. To find solitary wave solution is the basic aim for the investigation of NLEEs. There are some well-known NLEEs have been discussed in literature like Schrödinger equation, 2D Ginzburg-Landau equation, Phi-4 equation, model of blood flow in arteries, Zakharov-system, shallow water equations, diffusive predator prey system etc. Cubic complex Ginzburg-Landau equation (CCGLE) [13],

$$i\phi_t - \frac{D}{2}\phi_{xx} + \mid \phi \mid^2 \phi = i\delta\phi + i\beta\phi_{xx} + i\varepsilon \mid \phi \mid^2 \phi + i\mu \mid \phi \mid^4 \phi, \tag{1.3.2}$$

Non-linear coupled Boussinesq equation [37],

$$iE_t + E_{xx} + \beta_1 E - NE = 0, \tag{1.3.3}$$

$$3N_{tt} - N_{xxxx} + 3(N^2)_{xx} + \beta_2 N_{xx} - (| E |^2)_{xx} = 0 \tag{1.3.4}$$

Paraxial NLSE whose dimensionless form is given, as [39]:

$$iq_z + \frac{\alpha}{2} q_{tt} + \frac{\beta}{2} q_{yy} + \gamma(| q |^2)q = 0. \tag{1.3.5}$$

Phi-four equation,

$$u_{tt} - u_{xx} + m^2 u + \lambda u^3 = 0. \tag{1.3.6}$$

Cubic-quartic NLSE [38],

$$iq_t + iaq_{xxx} + bq_{xxxx} + F(| q |^2)q = 0. \tag{1.3.7}$$

The Benney-Luke equation,

$$u_{tt} - u_{xx} + \alpha u_{xxxx} - \beta u_{xxtt} + u_t u_{xx} + 2u_t u_{xt} = 0. \tag{1.3.8}$$

Diffusive predator prey system,

$$\frac{du}{dt} = uf(u) - g(u,v)v, \tag{1.3.9}$$

$$\frac{dv}{dt} = cg(u,v)v - \theta v. \tag{1.3.10}$$

These NLEEs possesses the soliton solutions with the special property that they conserve their shape and speed even after interacting with each other. Soliton solutions might be obtained from integrable NLEEs like KdV and NLSE. The accurate solutions of NLEEs also help us by providing documentation about the design of complex physical phenomena. Therefore, the investigation of solitary wave solutions for NLEEs shifts into an essential task in the research of nonlinear phenomena.

1.4 Fractional Calculus

Fractional calculus is the most important branch of mathematical analysis that investigates the distinct possibilities of real or complex exponents of derivative or integral operators. In 1695, it was first appeared is in a letter of l'Hospital written to Leibnitz. At the same time, Leibnitz wrote to one of the Bernoulli brothers to explain the similarity between the Leibnitz rule for the fractional derivative of a product of two functions and the binomial theorem. In one of Niels Henrik Abel's early papers, fractional calculus also discussed. In 1832, the foundations of the subject were laid by Liouville in his paper. In 1890, Oliver Heaviside introduced the applications of fractional differential operators in electrical transmission line analysis. The theory and applications of fractional calculus expanded greatly over the 19th and 20th centuries, and numerous contributors have given definitions for fractional derivatives and integrals. Nowadays, it is a growing field of mathematics that build out of the popular definitions of integral calculus and derivative operators. Various type of fractional derivatives has been studied, in which Riemann-Liouville, Caputo-Fabrizo, Atangana Baleanu and conformable fractional derivatives (CFD) are the most used ones [11, 12, 7, 10, 5, 3]. Some types of fractional derivatives at $(n-1 \leq \beta < n)$.

Riemann–Liouvill fractional derivative,

$$ {}_aD_t^{\beta} g(t) = \frac{1}{\Gamma(n-\beta)} \left(\frac{d}{dt}\right)^n \int_a^t \frac{g(\xi)d\xi}{(t-\xi)^{\beta-n+1}}. \tag{1.4.1}$$

Caputo–Fabrizio fractional derivative,

$$ {}_a^{CF}D_t^{\beta} g(t) = \frac{1}{1-\beta} \int_a^t g'(\xi) exp\left(-\beta \frac{t-\xi}{1-\beta}\right) d\xi. \tag{1.4.2}$$

Hadamard fractional derivative,

$$ {}_aD_t^{-\beta} g(t) = \frac{1}{\Gamma(\beta)} \int_a^t \left(log \frac{t}{\xi}\right)^{\beta-1} g(\xi) \frac{d\xi}{\xi}, \qquad t > \beta. \tag{1.4.3}$$

Caputo-Katugampola fractional derivative,

$$
\begin{aligned}
{}^{C}D_{a^+}^{\beta,\rho} g(t) &= \frac{\rho^{\beta} t^{1-\beta}}{\Gamma(1-\beta)} \frac{d}{dt} \int_a^t \frac{v^{\rho-1}}{(t^{\rho}-v^{\rho})^{\beta}} [g(v)-g(a)] dv, \\
&\text{or} \\
&= \frac{\rho^{\beta}}{\Gamma(1-\beta)} \int_a^t \frac{g'(v)}{(t^{\rho}-v^{\rho})^{\beta}} dv. \qquad (1.4.4)
\end{aligned}
$$

Atangana-Baleanu fractional derivative,

$$
{}^{ABD}D_{a^+}^{\beta} g(t) = \frac{F(\beta)}{1-\beta} \frac{d}{dt} \int_a^t g(x) \wp_{\beta} \left(\frac{-\beta (t-\beta)^{\beta}}{1-\beta} \right) dx, \qquad (1.4.5)
$$

where $\wp_{\beta}$ is Mittag–Leffler function and $F(\beta)$ is a normalize function.

1.5 Summary of the Sine-cosine, Cosech and tan-cot method

To obtain the various type of solitons we will use following assumptions.

We will assume following transformation to get bell type solitons for Sine-cosine method.

$$
u(x,t) = \lambda sin^{\beta}(\mu x) e^{i\varphi t}. \qquad (1.5.1)
$$

The transformation to retrieve kink and anti-kink type solitons for Tan-cot approach.

$$
u(x,t) = tan^{\sigma}(\upsilon x) e^{i\varphi t}. \qquad (1.5.2)
$$

For Cosech technique we will use following assumption to get singular soliitons.

$$
u(x,t) = Acosech^{\alpha}(\tau x) e^{i\varphi t}. \qquad (1.5.3)
$$

where , A, B are the amplitudes of the wave and μ, υ, τ are the velocities of the wave and φ is phase shift.

After replacing these substitutions in NLEEs and using homogenous balance, we get a system of equations, then we find the unknown parameters. After that we replace these parameters to the original substitutions to get exact solutions of governing model.

1.6 Summary of the RPSM

In 2013, RPSM was proposed by Arqub and this is a unique scheme to obtain the power series solutions of NLPDEs. By the given initial conditions, RPSM provides approximate analytical solutions of the given NLPDE in truncated series with the help of residual function.
To obtain the power series solution of fractional order NLPDEs by using RPSM, we suppose following assumption.

$$Dv(x,t) = N(v) + R(v), \tag{1.6.1}$$

where $R(v)$ and $N(v)$ are the linear and nonlinear terms with the following initial condition,

$$v(x,0) = g(x). \tag{1.6.2}$$

At initial point, the RPSM define power series solution as given,

$$v(x,t) = g_0(x) + \Sigma_{n=1}^{\infty} g_n(x) \frac{t^{\beta}}{\Gamma(1+n\beta)}, \tag{1.6.3}$$

Where $0 < \beta < 1$, $-\infty < x < \infty$, $0 < t < R$.
Further we assume $m^t h$ truncated series of $v(x,t)$ is $v_m(x,t)$.

$$v_m(x,t) = g_0(x) + \Sigma_{n=1}^{m} g_n(x) \frac{t^{\beta}}{\Gamma(1+n\beta)}, \quad m = 1,2,3,... \tag{1.6.4}$$

The 0^{th} RPS approximate solution of $v(x,t)$ is.

$$v_0(x,t) = v(x,0) = g(x). \tag{1.6.5}$$

Now above equation can be written as,

$$v_m(x,t) = g_(x) + \Sigma_{n=1}^{m} g_n(x)\frac{t^{\beta}}{\Gamma(1+n\beta)}, \quad m = 1,2,3,... \tag{1.6.6}$$

Residual function is defined as.

$$Res_v(x,t) = D_t^{\beta} v(x,t) - N(v) - R(v). \tag{1.6.7}$$

Its m^{th} residual function $Res_(v,m)(x,t)$.

$$Res_{v,m}(x,t) = D_t^{\beta} v_m(x,t) - N(v_m) - R(v_m). \tag{1.6.8}$$

Therefore,

$$D_t^{n\beta} Res(x,0) = D_t^{n\beta} Res_m(x,0) = 0, \quad n = 0,1,2,,m. \tag{1.6.9}$$

To eliminate the value of $g_1(x)$, $g_2(x)$, $g_3(x)$,,. We consider $m = 1,2,3,$ and applying fractional derivative $D_t^{(m-1)\beta}$ on both sides, $m = 1,2,3,$ and then compute $D_t^{(m-1)\beta} Res_(v,m)(x,0) = 0$.

1.7 Summary of the Sub-ode technique

To approach this sub ode, we suppose the following solution: [28, 29]

$$G(\eta) = \mu M^m(\eta), \quad \mu > 0 \tag{1.7.1}$$

here m is a parameter and $M(\eta)$ satisfies the equation:

$$M'^2(\eta) = \Upsilon M^{2-2p}(\eta) + \Delta M^{2-p}(\eta) + \Lambda M^2(\eta) + \Pi M^{2+p}(\eta) + \Psi M^{2+2p}(\eta), \ p > 0, \tag{1.7.2}$$

here $\Upsilon, \Delta, \Lambda, \Pi$ *and* Ψ are constants. By using homogeneous balance method we can find m in Eq. (1.7.1) given as ,

$$D(\phi_1) = m, \;\; D(\phi^2) = 2m, , ... \;\; D(\phi') = m + p, \;\; D(\phi'') = m + 2p, ... \tag{1.7.3}$$

Thus Eq. (1.7.2) has following solutions cases:

Case 1: When $\Upsilon = \Delta = \Pi = 0$, we have a bell type soliton solution for Eq. (1.7.2) as:

$$G(\eta) = \left[\sqrt{-\frac{\Lambda}{\Psi}} \sec h(\sqrt{\Lambda} p\eta)\right]^{\frac{1}{p}}, \quad \Lambda > 0, \;\; \Psi < 0, \tag{1.7.4}$$

a periodic solution

$$G(\eta) = \left[\sqrt{-\frac{\Lambda}{\Psi}} \sec(\sqrt{-\Lambda} p\eta)\right]^{\frac{1}{p}}, \quad \Lambda < 0, \;\; \Psi > 0, \tag{1.7.5}$$

and a rational solution

$$G(\eta) = \left[\frac{\varepsilon}{\sqrt{\Psi} p\eta}\right]^{\frac{1}{p}}, \quad \Lambda = 0, \;\; \Psi > 0, \;\; \varepsilon = \pm 1. \tag{1.7.6}$$

Case 2: If $\Delta = \Pi = 0$, $\Upsilon = \frac{\Lambda^2}{4\Psi}$, then Eq. (1.7.2) has a kink type soliton:

$$G(\eta) = \left[\varepsilon\sqrt{-\frac{\Lambda}{\Psi}} \tanh(\sqrt{\Lambda} p\eta)\right]^{\frac{1}{p}}, \quad \Lambda > 0, \;\; \Psi < 0, \;\; \varepsilon = \pm 1, \tag{1.7.7}$$

and a periodic solution

$$G(\eta) = \left[\varepsilon\sqrt{-\frac{\Lambda}{\Psi}} \tan(\sqrt{-\Lambda} p\eta)\right]^{\frac{1}{p}}, \quad \Lambda < 0, \;\; \Psi > 0, \;\; \varepsilon = \pm 1, \tag{1.7.8}$$

Case 3: If $\Delta = \Pi = 0$, then Eq. (1.7.2) has following three JEF solutions:

$$G(\eta) = \left[\sqrt{-\frac{\Lambda m^2}{\Psi(2m^2 - 1)}} cn\left(\sqrt{\frac{\Lambda}{(2m^2 - 1)}} p\eta\right)\right]^{\frac{1}{p}}, \quad \Lambda > 0, \quad \Upsilon = \frac{\Lambda^2 m^2 (m^2 - 1)}{\Psi(2m^2 - 1)^2}, \tag{1.7.9}$$

$$G(\eta)=\left[\sqrt{-\frac{\Lambda}{\Psi(2-m^2)}}dn\left(\sqrt{\frac{\Lambda}{(2-m^2)}}p\eta\right)\right]^{\frac{1}{p}},\quad \Lambda>0,\quad \Upsilon=\frac{\Lambda^2(1-m^2)}{\Psi(2-m^2)^2},\tag{1.7.10}$$

and

$$G(\eta)=\left[\sqrt{-\frac{\Lambda m^2}{\Psi(m^2+1)}}sn\left(\sqrt{-\frac{\Lambda}{(m^2+1)}}p\eta\right)\right]^{\frac{1}{p}},\quad \Lambda<0,\quad \Upsilon=\frac{\Lambda^2 m^2}{\Psi(m^2+1)^2}.\tag{1.7.11}$$

Case 6: For $\Delta=\Pi=0$, the WEF solutions are obtained for Eq. (1.7.2) as:

$$G(\eta)=\left[\frac{1}{\Psi}\wp(p\eta,g_2,g_3)-\frac{\Lambda}{3}\right]^{\frac{1}{2p}},\tag{1.7.12}$$

where $g_2=\frac{4\Lambda^2}{3}$ and $g_3=\frac{4\Lambda(-2\Lambda^2)}{27}$.

$$G(\eta)=\frac{3\sqrt{\Psi-1}\wp'(p\eta,g_2,g_3)}{6\wp(p\eta,g_2,g_3)+\Lambda}^{\frac{1}{p}},\tag{1.7.13}$$

where $g_2=\frac{\Lambda 2}{12}$ *and* $g_3=0$.

Case 7: If $\Delta=\Pi=0$ and $\Upsilon=\frac{5\Lambda^2}{36\Psi}$ the Eq. (1.7.2) has following WEF solutions :

$$G(\eta)=\left[\frac{\Lambda\sqrt{\frac{-15\Lambda}{2\Psi}}\wp(p\eta,g_2,g_3)}{3\wp(p\eta,g_2,g_3)+\Lambda}\right]^{\frac{1}{p}},\tag{1.7.14}$$

where $g_2=\frac{2\Lambda^2}{9}$ and $g_3=\frac{\Lambda^3}{54}$. Here g_2 and g_3 are known as invariant WEF.

Case 8: For $\Upsilon=\Delta=0$, the following bell type and kink type solutions for Eq. (1.7.2) are obtained:

$$G(\eta)=\left(\frac{1}{\cosh(\sqrt{\Lambda}p\eta)}\right)^{\frac{1}{p}},\;\; \Lambda>0,\;\; \Pi=0,\;\; \Psi=\frac{\Pi^2}{4\Lambda}-\Lambda,\tag{1.7.15}$$

$$G(\eta)=\left(\frac{1}{2}\sqrt{\frac{\Lambda}{\Psi}}\left[1+\varepsilon\tanh\left(\frac{1}{2}\sqrt{\Lambda}p\eta\right)\right]\right)^{\frac{1}{p}},\;\; \Lambda>0,\;\; \Psi>0,\;\; \Pi=0,\;\; \varepsilon=\pm1,\tag{1.7.16}$$

and

$$G(\eta)=\left(\frac{1}{(\frac{1}{2}p\eta)^2-\Psi}\right)^{\frac{1}{p}},\ \ \Lambda=0,\ \ \Pi=0,\ \ \Psi=<0. \tag{1.7.17}$$

Case 9: For$\Upsilon=\Delta=0,\Lambda>0$,then the following hyperbolic functions solutions for Eq. (1.7.2) are obtained:

$$G(\eta)=\Big[\frac{2\Lambda\sec h^2(\frac{\sqrt{\Lambda}}{2}p\eta)}{[\sqrt{-4\Lambda\Psi}]\sec h^2(\frac{\sqrt{\Lambda}}{2}p\eta)-2\sqrt{-4\Lambda\Psi}}]^{\frac{1}{p}}\ \ ,\ \ \Pi^2-4\Lambda\Psi>0 \tag{1.7.18}$$

$$G(\eta)=\left(\frac{2\Lambda\csc h^2(\frac{\sqrt{\Lambda}}{2}p\ \eta)}{[\sqrt{-4\Lambda\Psi}]\csc h^2(\frac{\sqrt{\Lambda}}{2}p\eta)+2\sqrt{-4\Lambda\Psi}}\right)^{\frac{1}{p}}\ \ ,\ \ \Pi^2-4\Lambda\Psi>0 \tag{1.7.19}$$

Case 10: For$\Upsilon=\Delta=0,\Lambda<0$,then the following periodic functions solutions for Eq. (1.7.2) are obtained:

$$G(\eta)=\left(\frac{2\Lambda\sec^2(\frac{\sqrt{-\Lambda}}{2}p\ \eta)}{[\sqrt{-4\Lambda\Psi}]\sec^2(\frac{\sqrt{-\Lambda}}{2}p\ \eta)-2\sqrt{-4\Lambda\Psi}}\right)^{\frac{1}{p}}\ \ ,\ \ \Pi^2-4\Lambda\Psi>0 \tag{1.7.20}$$

$$G(\eta)=\left(\frac{2\Lambda\csc^2(\frac{\sqrt{-\Lambda}}{2}p\ \eta)}{[\sqrt{-4\Lambda\Psi}]\csc^2(\frac{\sqrt{-\Lambda}}{2}p\ \eta)-2\sqrt{-4\Lambda\Psi}}\right)^{\frac{1}{p}}\ \ ,\ \ \Pi^2-4\Lambda\Psi>0 \tag{1.7.21}$$

1.8 Literature review

Many authors studied NLEEs for various kinds of soliton solutions. Mirzazadeh et al. [13] obtained the OS with complex Ginzburg-Landau equation. Wazwaz employed sine-cosine approach to obtain various types of dromions for non linear wave equation. They also used the same technique for obtaining diverse forms of solitons having both compact and non-compact characteristics [15]. Belic et al. [16] obtained OS in nonlinear directional couplers by Bernoullis equation approach Biswas and Triki [17] studied the OS for cubic-quartic NLSE with Kerr law and non Kerr nonlinearities. Anwar et al. retrieved singular solitons for the Kaup Newell equation by using cosech method [32]. Jawad and Anwar obtained dark solitons solution of space-time Bogoyavlenskii and Konopelchenko Dubrovsky coupled system with the aid of tan-cot method [33]. Dubey et al. worked on time-fractional NLEE with the aid of RPSM [20].

Mahmood et al. compared the analytical and numerical solutions of Boussinesq-Burgers equation using RPSM [21]. Chen et al. achieved the solution of NLEEs with variable coefficients by using power series method [22]. Arafa et al. worked on fractional coupled physical equations with help of same technique [23]. Alka et al. retrieved chirped and chirped free solitons of cubic quintic NLSE with self frequency shift [40]. Triki et al. applied the sub-ode scheme on NLSE with continuous wave background to compute the chirped solitons [41]. Using sub-ode approach, Zayeda et al. computed the chirped and chirped free solitons for Bragg equation [42]. Ghanbari and Atangana studied some applications of ABFD in image processing [24]. Jarad et al. studied uniqueness and existence conditions for numerous ordinary differential equations with ABFD [25]. Owolabi displayed relationship between dynamical system and ABFD [26]. Peter et al. used AB Operator to analyse fractional order mathematical model of COVID-19 in Nigeria [27]

Chapter 2

Bell type, Kink and Anti-kink type, Power series solutions for CIMA chemical equations

In 1990, the first practical observation of a Turing pattern in a chemical reactor was observed by De Keppers group, who observed a spotty pattern in a CIMA reaction. The $ClO_2 - I - MA$ reaction (CIMA) is chemically described as follow:

$$\begin{aligned} MA + I_2 &\rightarrow IMA + I^- + H^+ \\ ClO_2 + I^- &\rightarrow ClO_2^- + \frac{1}{2} I_2 \\ ClO_2^- + 4I^- + 4H^+ &\rightarrow CL^- + 2I_2 + 2H_2O \end{aligned}$$

In open gel reactors, the practical on the CIMA reaction has elaborated the existence of stationary space periodic concentration patterns known as turing structures. Later, Lengyel and Epstein [30] proposed that due to the iodine activator species formed a reversible complex of low mobility where these patterns could arise. Particularly, they have also developed [31] a simple two-variable model known as CIMA model. The corresponding dimensionless CIMA chemical equation have following form:

$$u_t - u_{xx} - 5\alpha + u + \frac{4uv}{1+u^2} = 0, \quad x \in \Lambda, t > 0, \tag{2.0.1}$$

$$v_t - m(v_{xx} + u - \frac{uv}{1+u^2}) = 0, \quad x \in \Lambda, t > 0, \tag{2.0.2}$$

where Λ is a connected domain in R^n, $(n \geq 1)$, with smooth boundary $\partial\Lambda$. Our aim is to find exact and numerical solutions for LE system of CIMA chemical equations by applying four methods, namely sin-cosine method (SCM), cosech technique, tan-cot approach and RPSM in this chapter. SCM is applicable to get bell type soliton, cosech method gives singular, tan-cot scheme provides kink type solution and RPSM is applied to get power series solution.

We assume the following transformation,

$$u(x,t) = U(\xi), \quad v(x,t) = V(\xi), \quad \xi = x - ct. \tag{2.0.3}$$

After substituting in Eq. (2.0.1) and Eq. (2.0.2), we have,

$$-cU - cU^3 - U'' - U''U^2 - 5\alpha(1+U^2) + U + U^3 + 4UV = 0, \tag{2.0.4}$$

$$-cV - cVU^2 - m(V'' + V''U^2 + U + U^3 - UV) = 0. \tag{2.0.5}$$

2.1 SCM

Now, we assume following assumption for Eq. (2.0.4) and Eq. (2.0.5)[16],

$$U(\xi) = \lambda \cos^{\beta}(\mu\xi), \quad V(\xi) = \gamma \cos^{n}(\mu\xi), \tag{2.1.1}$$

By using Eq. (2.1.1) into Eq. (2.0.4) and Eq. (2.0.5) and comparing the coefficients of least power and highest nonlinear term of $\cos(\mu\xi)$, we get $\beta = -1$, $n = -1$ and following set of algebraic equations:

$$\lambda^3(1-c) + 2\mu^2\lambda = 0, \tag{2.1.2}$$

$$-c\lambda + \lambda = 0, \tag{2.1.3}$$

$$-2m\gamma\mu^2 = -m\lambda^3, \tag{2.1.4}$$

$$-c\lambda = -m\lambda, \tag{2.1.5}$$

$$-c\gamma\lambda^2 = m\gamma\lambda, \tag{2.1.6}$$

After solving these equations, we get

$$\mu = \sqrt{\frac{\lambda^2(c-1)}{2}}, \;\; \lambda = \frac{-m}{c}, \;\; \gamma = \frac{-m^2}{c^2},$$

Thus, we get

$$u(x,t) = \frac{-m}{c} sech(\sqrt{\frac{\lambda^2(c-1)}{2}}(x-ct)), \tag{2.1.7}$$

and

$$v(x,t) = \frac{-m^2}{c^2} sech(\sqrt{\frac{\lambda^2(c-1)}{2}}(x-ct)). \tag{2.1.8}$$

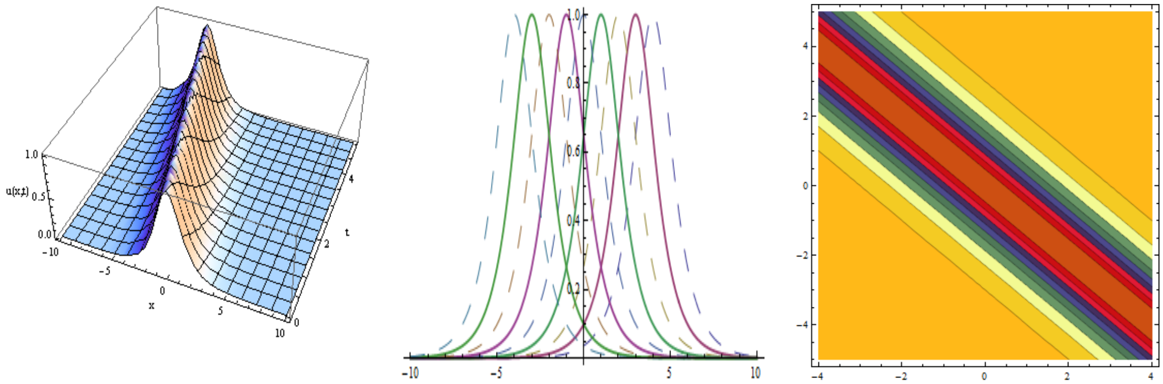

(a) (b) (c)

Figure 2.1: Graphical representation of $u(x,t)$ for Eq. (2.1.7) (a) shows 3-D graph x ∈ [-10, 10] and t ∈ [0, 5], (b) express 2-D plot in [-10, 10] and [0, 1.0], (c) express contour plot in [-4, 4] and [-4, 4].

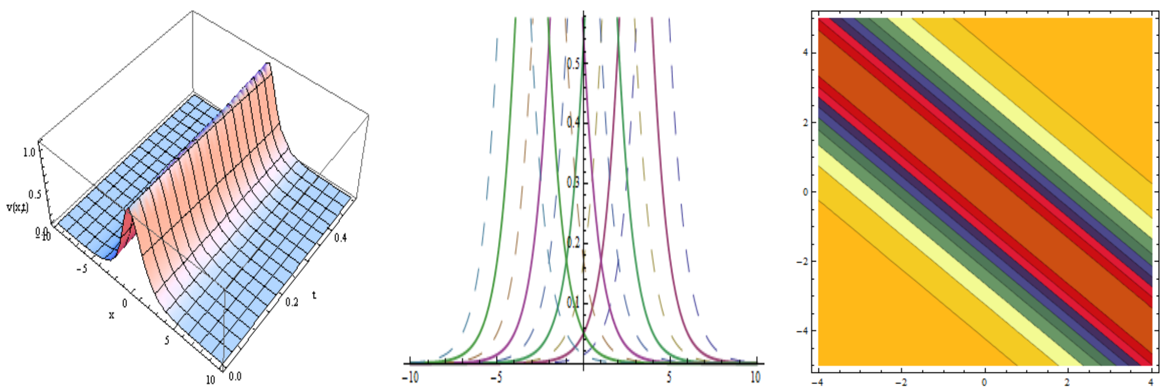

(a) (b) (c)

Figure 2.2: Graphical representation of $v(x,t)$ for Eq. (2.1.8) (a) shows 3-D graph x ∈ [-10, 10] and t ∈ [0, 5], (b) express 2-D plot in [-10, 10] and [0, 1.0], (c) express contour plot in [-4, 4] and [-4, 4].

2.2 Csch method

Now, we assume the following transformation [32],

$$U(\xi) = Acsch^{\tau}(\eta\xi), \quad V(\xi) = Bcsch^{\gamma}(\eta\xi), \tag{2.2.1}$$

After putting into Eq. (2.0.4) and Eq. (2.0.5) and comparing the coefficients of least power and highest nonlinear term of $csch(\mu\xi)$, then we get $\tau = 1$, $\gamma = 1$ and the following set of algebraic equations:

$$-cA + A - A\eta^2 = 0, \tag{2.2.2}$$

$$-2A\eta^2 = A^3(1-c), \tag{2.2.3}$$

$$-cA^2B - mA^3 = 0, \tag{2.2.4}$$

$$-mA - cB = 0, \tag{2.2.5}$$

$$-2mB\eta^2 + mAB = 0, \tag{2.2.6}$$

After solving above equations, we get

$$\eta = \sqrt{c-1}, \ A = \sqrt{\frac{2\eta^2}{c-1}}, \ B = \frac{-m}{c}\sqrt{\frac{2\eta^2}{c-1}}$$

Hence, we get

$$u(x,t) = \sqrt{\frac{2\eta^2}{c-1}} csch(\sqrt{c-1}(x-ct)), \tag{2.2.7}$$

and

$$v(x,t) = \frac{-m}{c}\sqrt{\frac{2\eta^2}{c-1}} csch(\sqrt{c-1}(x-ct)). \tag{2.2.8}$$

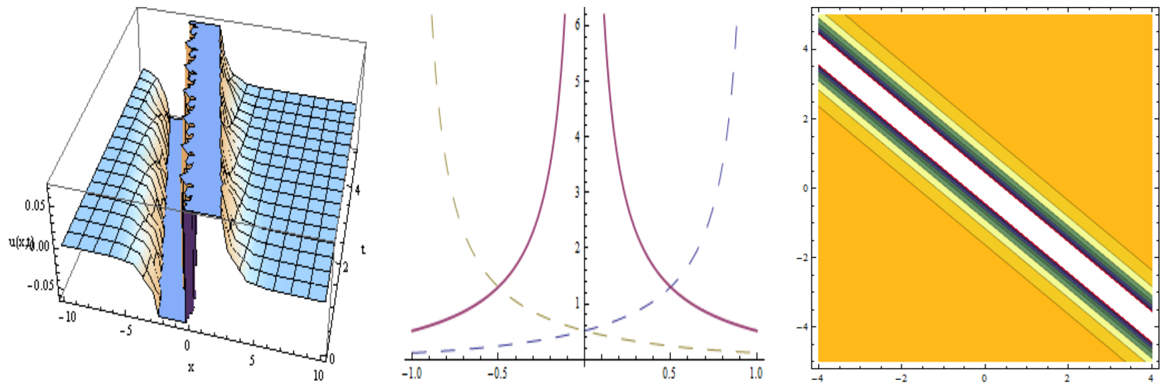

(a) (b) (c)

Figure 2.3: Graphical representation of $u(x,t)$ for Eq. (2.2.7) (a) shows 3-D graph x $\in$ [-10, 10] and t $\in$ [0, 5], (b) express 2-D plot in [-10, 10] and [0, 1.0], (c) express contour plot in [-4, 4] and [-4, 4].

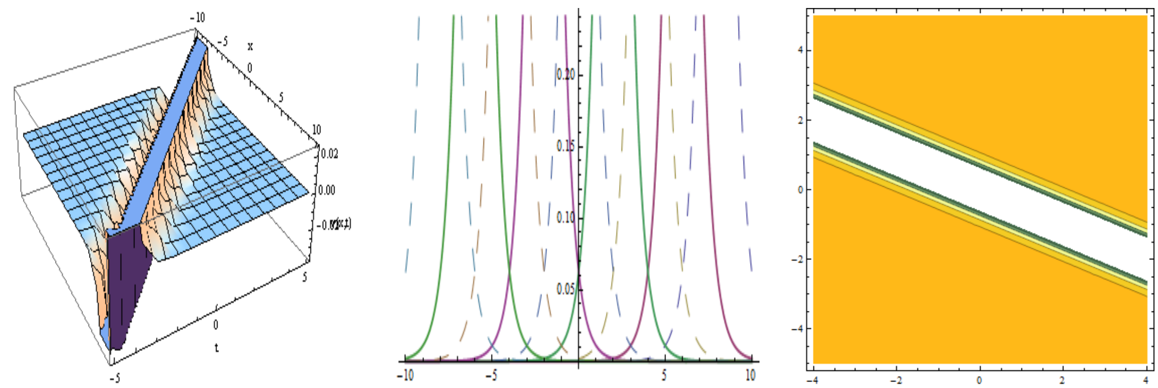

(a) (b) (c)

Figure 2.4: Graphical representation of $v(x,t)$ for Eq. (2.2.8) (a) shows 3-D graph x $\in$ [-10, 10] and t $\in$ [0, 5], (b) express 2-D plot in [-10, 10] and [0, 1.0], (c) express contour plot in [-4, 4] and [-4, 4].

2.3 $\tan - \cot$ method

Here we consider the following transformation [33],

$$U(\xi) = C\tan^{\beta}(\mu\xi), \quad V(\xi) = D\tan^{\gamma}(\mu\xi), \tag{2.3.1}$$

Using above transformation into Eq. (2.0.4) and Eq. (2.0.5) and comparing the coefficients of least power and highest nonlinear term of $\tan(\mu\xi)$, then we get $\beta = 2$, $\gamma = 4$ and following set of algebraic equations:

$$2C^3\mu^2 = -5\alpha C^2, \tag{2.3.2}$$

$$-cC + \lambda = 0, \tag{2.3.3}$$

$$C(1-c) = -8C\mu^2, \tag{2.3.4}$$

$$-cD - 16D\mu^2 = 0, \tag{2.3.5}$$

After solving above equations, we get

$$\mu = \sqrt{\frac{(c-1)}{8}},\ \ C = \frac{-5\alpha}{2\mu^2},\ \ D = \frac{(1-c)(\frac{-5\alpha}{2\mu^2})^2}{4}$$

.

Finally, we get

$$u(x,t) = \frac{-5\alpha}{2\mu^2}\tanh^2(\sqrt{\frac{(c-1)}{8}}(x-ct)), \tag{2.3.6}$$

and

$$v(x,t) = \frac{(1-c)(\frac{-5\alpha}{2\mu^2})^2}{4}\tanh^4(\sqrt{\frac{(c-1)}{8}}(x-ct)). \tag{2.3.7}$$

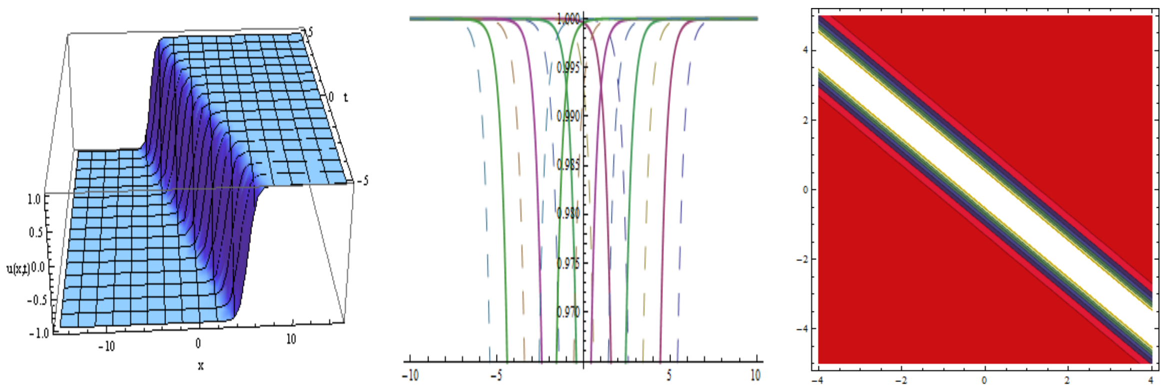

(a) (b) (c)

Figure 2.5: Graphical representation of $u(x,t)$ for Eq. (2.3.6) (a) shows 3-D graph x $\in$ [-10, 10] and t $\in$ [0, 5], (b) express 2-D plot in [-10, 10] and [0, 1.0], (c) express contour plot in [-4, 4] and [-4, 4].

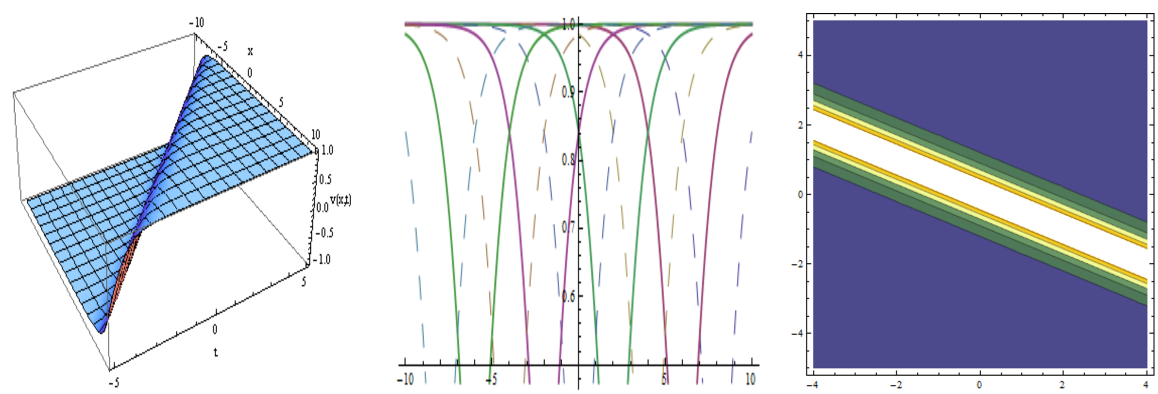

(a) (b) (c)

Figure 2.6: Graphical representation of $v(x,t)$ for Eq. (2.3.7) (a) shows 3-D graph x $\in$ [-10, 10] and t $\in$ [0, 5], (b) express 2-D plot in [-10, 10] and [0, 1.0], (c) express contour plot in [-4, 4] and [-4, 4].

2.4 RPSM method

Consider the LE system of CIMA chemical reaction,

$$D_t^{\alpha}u - u_{xx} - 5\alpha + u + \frac{4uv}{1+u^2} = 0, \tag{2.4.1}$$

$$D_t^{\alpha}v - m(v_{xx} + u - \frac{uv}{1+u^2}) = 0. \tag{2.4.2}$$

subject to the initial conditions.

$$u(x,0) = f_0(x), \tag{2.4.3}$$

$$v(x,0) = g_0(x). \tag{2.4.4}$$

We define a residual function for Eq. (2.4.1) and Eq. (2.4.2) as

$$Res_u(x,t) = D_t^{\alpha} u - u_{xx} - 5\alpha + u + \frac{4uv}{1+u^2}, \tag{2.4.5}$$

$$Res_v(x,t) = D_t^{\alpha} v - m(v_{xx} + u - \frac{uv}{1+u^2}). \tag{2.4.6}$$

Therefore the kth residual function $Res_{u,k}(x,t)$ and $Res_{v,k}(x,t)$

$$Res_{u,k}(x,t) = D_t^{\alpha} u_k - u_{k,xx} - 5\alpha + u_k + \frac{4u_k v_k}{1+u_k^2}, \tag{2.4.7}$$

$$Res_{v,k}(x,t) = D_t^{\alpha} v_k - m(v_{k,xx} + u_k - \frac{u_k v_k}{1+u_k^2}). \tag{2.4.8}$$

Let us consider the series solution,

$$u_k(x,t) = f_0(x) + \Sigma_{n=1}^{k} f_n(x) \frac{t^{\alpha}}{\Gamma(1+n\alpha)}, \tag{2.4.9}$$

$$v_k(x,t) = g_0(x) + \Sigma_{n=1}^{k} g_n(x) \frac{t^{\alpha}}{\Gamma(1+n\alpha)}. \tag{2.4.10}$$

To find the f_1 and g_1 put $k = 1$, then

$$u_1(x,t) = f_0(x) + f_1(x) \frac{t^{\alpha}}{\Gamma(1+\alpha)}, \tag{2.4.11}$$

$$v_1(x,t) = g_0(x) + g_1(x) \frac{t^{\alpha}}{\Gamma(1+\alpha)}. \tag{2.4.12}$$

$$Res_{u,1}(x,t) = D_t^{\alpha} u_1 - u_{1,xx} - 5\alpha + u_1 + \frac{4u_1 v_1}{1+u_1^2}, \tag{2.4.13}$$

$$Res_{v,1}(x,t) = D_t^{\alpha} v_1 - m(v_{1,xx} + u_1 - \frac{u_1 v_1}{1+u_1^2}). \tag{2.4.14}$$

now inserting Eq. (2.4.11) and Eq. (2.4.12) into Eq. (2.4.13) and Eq. (2.4.14) respectively, we get

$$\begin{aligned} Res_{u,1}(x,t) = f_1(x) - (f_0''(x) + f_1''(x)\frac{t^{\alpha}}{\Gamma(1+\alpha)}) - 5\alpha + (f_0(x) + f_1(x)\frac{t^{\alpha}}{\Gamma(1+\alpha)}) \\ + \frac{4(f_0(x) + f_1(x)\frac{t^{\alpha}}{\Gamma(1+\alpha)})(g_0(x) + g_1(x)\frac{t^{\alpha}}{\Gamma(1+\alpha)})}{1 + (f_0(x) + f_1(x)\frac{t^{\alpha}}{\Gamma(1+\alpha)})^2}, \end{aligned}$$

$$\begin{aligned} Res_{v,1}(x,t) = g_1(x) - m(g_0''(x) + g_1''(x)\frac{t^{\alpha}}{\Gamma(1+\alpha)}) + (g_0(x) + g_1(x)\frac{t^{\alpha}}{\Gamma(1+\alpha)}) \\ - \frac{(f_0(x) + f_1(x)\frac{t^{\alpha}}{\Gamma(1+\alpha)})(g_0(x) + g_1(x)\frac{t^{\alpha}}{\Gamma(1+\alpha)})}{1 + (f_0(x) + f_1(x)\frac{t^{\alpha}}{\Gamma(1+\alpha)})^2}. \end{aligned}$$

By given initial condition we have,

$$D_t^{(k-1)\alpha} u_k(x,0) = 0, \tag{2.4.15}$$

$$D_t^{(k-1)\alpha} v_k(x,0) = 0. \tag{2.4.16}$$

$$f_1(x) = f_0''(x) + 5\alpha - f_0(x) - \frac{f_0(x) g_0(x)}{1 + f_0^2(x)}, \tag{2.4.17}$$

$$g_1(x) = m(g_0''(x) + f_0(x) - \frac{f_0(x) g_0(x)}{1 + f_0^2(x)}). \tag{2.4.18}$$

Similarly, we can find higher order terms by putting $k = 2, 3, 4, \ldots$. Thus Eq. (2.4.11) and Eq. (2.4.12) becomes,

$$u_1(x,t) = f_0(x) + (f_0''(x) + 5\alpha - f_0(x) - \frac{f_0(x)g_0(x)}{1+f_0^2(x)})\frac{t^\alpha}{\Gamma(1+\alpha)}, \tag{2.4.19}$$

$$v_1(x,t) = g_0(x) + (m(g_0''(x) + f_0(x) - \frac{f_0(x)g_0(x)}{1+f_0^2(x)}))\frac{t^\alpha}{\Gamma(1+\alpha)}. \tag{2.4.20}$$

Case 1:

$$u(x,0) = f_0(x) = \lambda sech(\sqrt{\frac{\lambda^2(c-1)}{2}}(x)), \tag{2.4.21}$$

$$v(x,0) = g_0(x) = \gamma sech(\sqrt{\frac{\lambda^2(c-1)}{2}}(x-ct)). \tag{2.4.22}$$

Now replacing the values of $f_0(x)$ and $g_0(x)$ in Eq. (2.4.19) and Eq. (2.4.20),

$$u_1(x,t) = \lambda sech(\sqrt{\frac{\lambda^2(c-1)}{2}}(x)) + (5\alpha - \frac{8\gamma\lambda}{1+2\lambda^2+\cosh(\lambda\sqrt{2-2c}x)} - \lambda sech(\sqrt{\frac{\lambda^2(c-1)}{2}}(x)) \tag{2.4.23}$$

$$+\frac{1}{2}(c-1)\lambda^3 sech(\sqrt{\frac{\lambda^2(c-1)}{2}}(x)) - 4(c-1)\lambda^3 cosech^3(\sqrt{\frac{\lambda^2(c-1)}{2}}(x))\sinh^5(\sqrt{\frac{\lambda^2(c-1)}{2}}(x)))\frac{t^\alpha}{\Gamma(1+\alpha)}, \tag{2.4.24}$$

$$v_1(x,t) = (\gamma + \frac{m\lambda}{2}(2+\gamma\lambda(c-1) - \frac{4\gamma\cosh(\sqrt{\frac{\lambda^2(c-1)}{2}}(x))}{1+2\lambda^2+\cosh(\lambda\sqrt{2-2c}x)})sech(\sqrt{\frac{\lambda^2(c-1)}{2}}(x)))\frac{t^\alpha}{\Gamma(1+\alpha)} \tag{2.4.25}$$

Case 2:

$$u(x,0) = f_0(x) = Acsch(\sqrt{c-1}(x)), \tag{2.4.26}$$

$$v(x,0) = g_0(x) = Bcsch(\sqrt{c-1}(x)). \tag{2.4.27}$$

Now by replacing the values of $f_0(x)$ and $g_0(x)$ in Eq. (2.4.19) and Eq. (2.4.20),

$$u_1(x,t) = A(csch[\sqrt{1-c}]x) + (5\alpha - Acsch[\sqrt{1-cx}] - (-1+c)A\coth[\sqrt{1-cx}]^2 csch[\sqrt{1-cx}] \tag{2.4.28}$$

$$-(-1+c)Acsch[\sqrt{1-cx}]^3 - \frac{4ABcsch[\sqrt{1-cx}]^2}{1+A^2csch[\sqrt{1-cx}]^2}\frac{t^\alpha}{\Gamma(1+\alpha)} \tag{2.4.29}$$

$$v_1(x,t) = Bcsch[\sqrt{1-cx}] + (Acsch[\sqrt{1-cx}] - (-1+c)B\coth[\sqrt{1-cx}]^2 csch[\sqrt{1-cx}] \tag{2.4.30}$$

$$-(-1+c)Bcsch[\sqrt{1-cx}]^3 - \frac{ABcsch[\sqrt{1-cx}]^2}{1+A^2csch[\sqrt{1-cx}]^2}\frac{t^\alpha}{\Gamma(1+\alpha)} \tag{2.4.31}$$

Case 3:

$$u(x,0) = f_0(x) = \lambda\tanh^2(\sqrt{\frac{(c-1)}{8}}(x)), \tag{2.4.32}$$

$$v(x,0) = g_0(x) = \gamma\tanh^4(\sqrt{\frac{(c-1)}{8}}(x)). \tag{2.4.33}$$

By replacing the values of $f_0(x)$ and $g_0(x)$ into Eq. (2.4.19) and Eq. (2.4.20),

$$u_1(x,t) = \lambda\tanh[\frac{(\sqrt{1-cx})}{(2\sqrt{2})}] + 5\alpha + 2(-1+c)\lambda csch[(\sqrt{1-cx})\sqrt{2}]^3\sinh[\frac{(\sqrt{1-cx})}{(2\sqrt{2})}]^4 - \lambda\tanh[\frac{\sqrt{1-cx}}{(2\sqrt{2})}] \tag{2.4.34}$$

$$-\frac{4\lambda\gamma\tanh^2[\frac{\sqrt{1-cx}}{2\sqrt{2}}]}{1+\lambda^2\tanh^2[\frac{(\sqrt{1-cx})}{2\sqrt{2}}]}\frac{t^\alpha}{\Gamma(1+\alpha)} \tag{2.4.35}$$

$$v_1(x,t) = \gamma\tanh[\frac{(\sqrt{1-cx})}{(2\sqrt{2})}] + [2(-1+c)\gamma csch^3[\frac{(\sqrt{1-cx})}{2\sqrt{2}}]\sinh^4[\frac{(\sqrt{1-cx})}{(2\sqrt{2})}] + \lambda\tanh[\frac{(\sqrt{1-cx})}{(2\sqrt{2})} \tag{2.4.36}$$

$$-\frac{\gamma\lambda\tanh^2[\frac{\sqrt{1-cx}}{2\sqrt{2}}]}{(1+\lambda^2\tanh^2[\frac{(\sqrt{1-cx})}{(\sqrt{2})}])}]\frac{t^\alpha}{\Gamma(1+\alpha)} \tag{2.4.37}$$

2.5 Results and Discussion

Now we will analyze our derived results in detail. In this work, we produced bell shaped, kink-type, singular soliton and power series solutions for CIMA chemical equations. sine-cosine approach provided bell shaped soliton, $\csc h$ technique gave singular soliton and $\tan - \cot$ method calculate kink-type soliton solution. We also obtained numerical solutions for our governing model with the aid of RPS architectonic. We classified the structure of our new obtained solutions, and shown our results in the form of 3-D, 2-D and contour graphs.

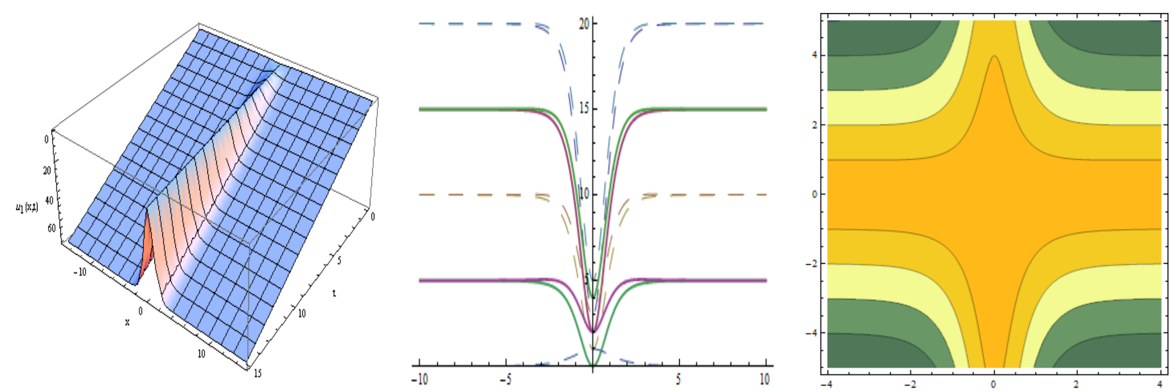

(a) (b) (c)

Figure 2.7: Graphical representation of $u_1(x,t)$ in Eq. (2.4.24) at $\alpha = 1$ (a) shows 3-D graph x $\in$ [-10, 10] and t $\in$ [0, 5], (b) express 2-D plot in [-10, 10] and [0, 1.0], (c) express contour plot in [-4, 4] and [-4, 4].

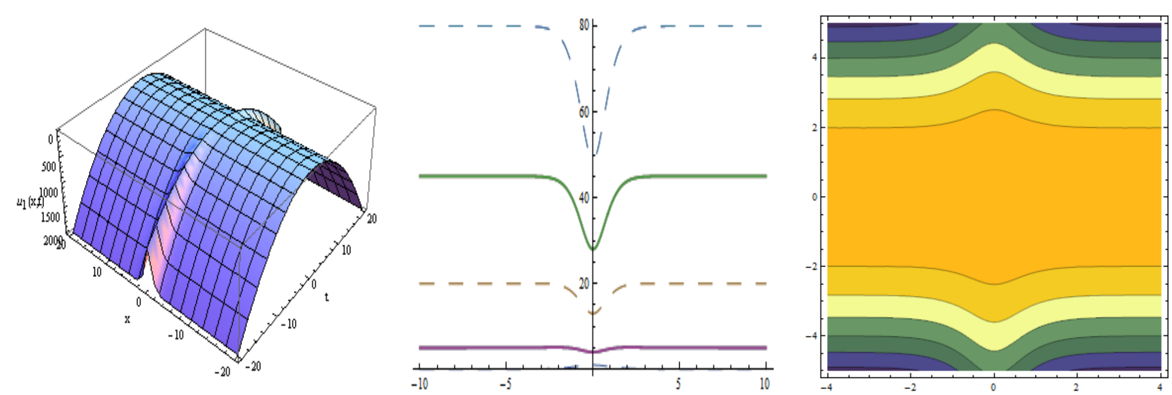

(a) (b) (c)

Figure 2.8: Graphical representation of $u_1(x,t)$ in Eq. (2.4.24) at $\alpha = 2$ (a) shows 3-D graph x $\in$ [-10, 10] and t $\in$ [0, 5], (b) express 2-D plot in [-10, 10] and [0, 1.0], (c) express contour plot in [-4, 4] and [-4, 4].

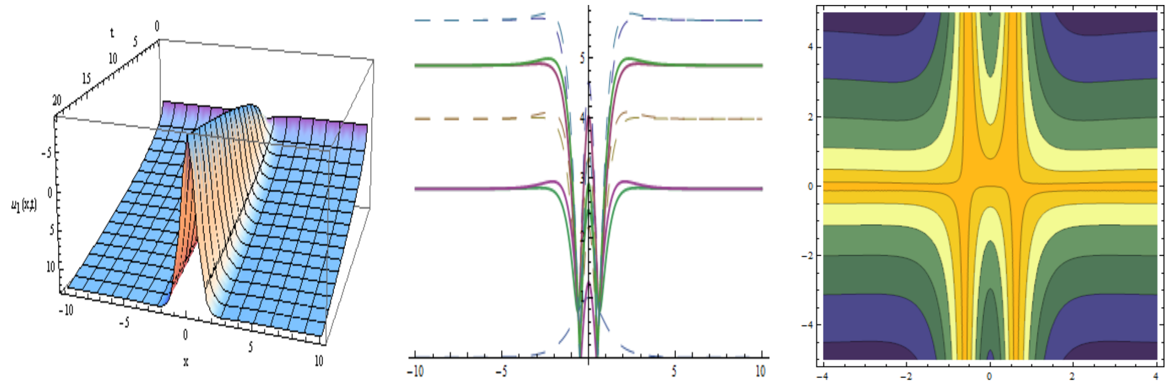

(a) (b) (c)

Figure 2.9: Graphical representation of $u_1(x,t)$ in Eq. (2.4.24) at $\alpha = \frac{1}{2}$ (a) shows 3-D graph x $\in$ [-10, 10] and t $\in$ [0, 5], (b) express 2-D plot in [-10, 10] and [0, 1.0], (c) express contour plot in [-4, 4] and [-4, 4].

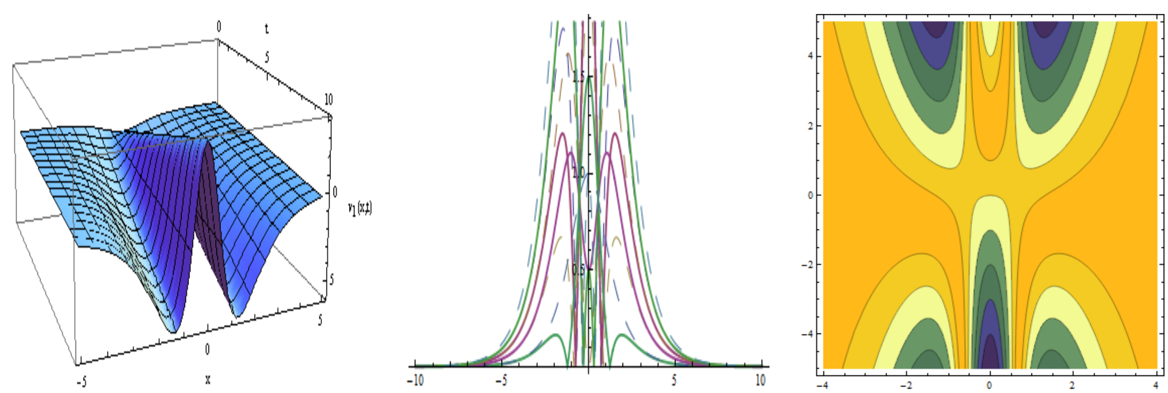

(a) (b) (c)

Figure 2.10: Graphical representation of $v_1(x,t)$ in Eq. (2.4.25) at $\alpha = 1$ (a) shows 3-D graph x $\in$ [-10, 10] and t $\in$ [0, 5], (b) express 2-D plot in [-10, 10] and [0, 1.0], (c) express contour plot in [-4, 4] and [-4, 4].

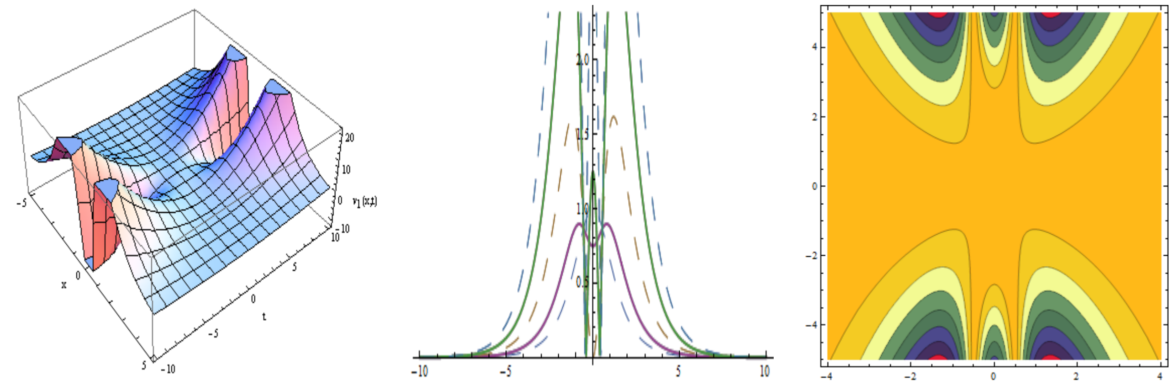

(a) (b) (c)

Figure 2.11: Graphical representation of $v_1(x,t)$ in Eq. (2.4.25) at $\alpha = 2$ (a) shows 3-D graph x $\in$ [-10, 10] and t $\in$ [0, 5], (b) express 2-D plot in [-10, 10] and [0, 1.0], (c) express contour plot in [-4, 4] and [-4, 4].

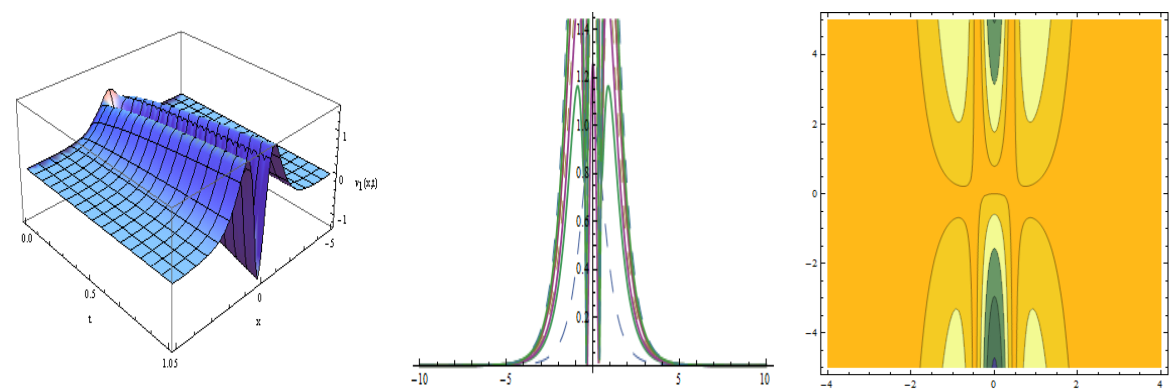

(a) (b) (c)

Figure 2.12: Graphical representation of $v_1(x,t)$ in Eq. (2.4.25) at $\alpha = \frac{1}{2}$ (a) shows 3-D graph x $\in$ [-10, 10] and t $\in$ [0, 5], (b) express 2-D plot in [-10, 10] and [0, 1.0], (c) express contour plot in [-4, 4] and [-4, 4].

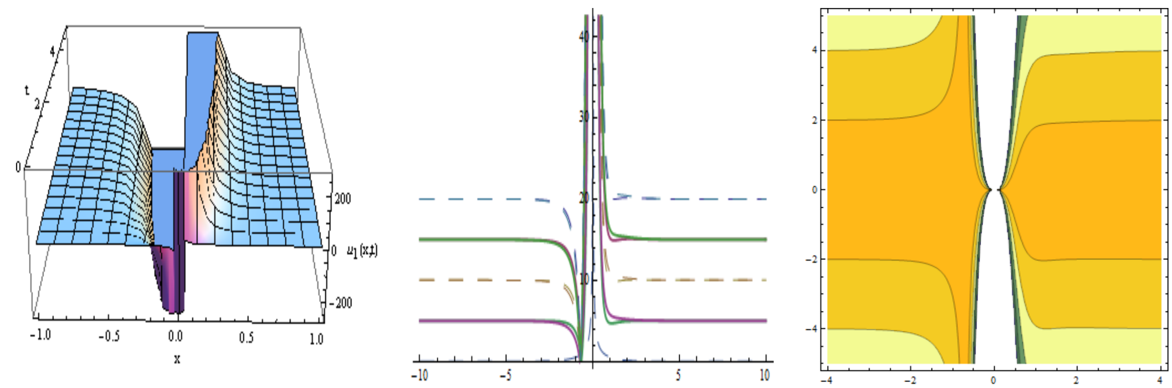

(a) (b) (c)

Figure 2.13: Graphical representation of $u_1(x,t)$ in Eq. (2.4.29) at $\alpha = 1$ (a) shows 3-D graph x $\in$ [-10, 10] and t $\in$ [0, 5], (b) express 2-D plot in [-10, 10] and [0, 1.0], (c) express contour plot in [-4, 4] and [-4, 4].

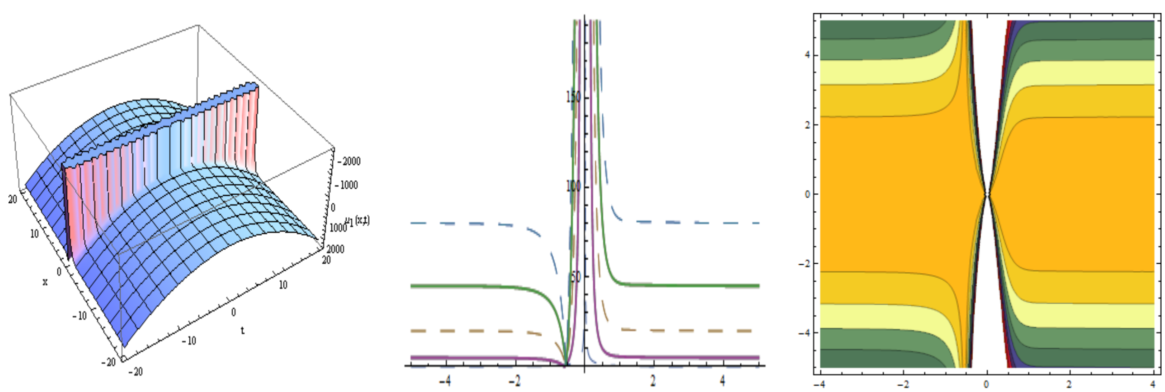

(a) (b) (c)

Figure 2.14: Graphical representation of $u_1(x,t)$ in Eq. (2.4.29) at $\alpha = 2$ (a) shows 3-D graph x $\in$ [-10, 10] and t $\in$ [0, 5], (b) express 2-D plot in [-10, 10] and [0, 1.0], (c) express contour plot in [-4, 4] and [-4, 4].

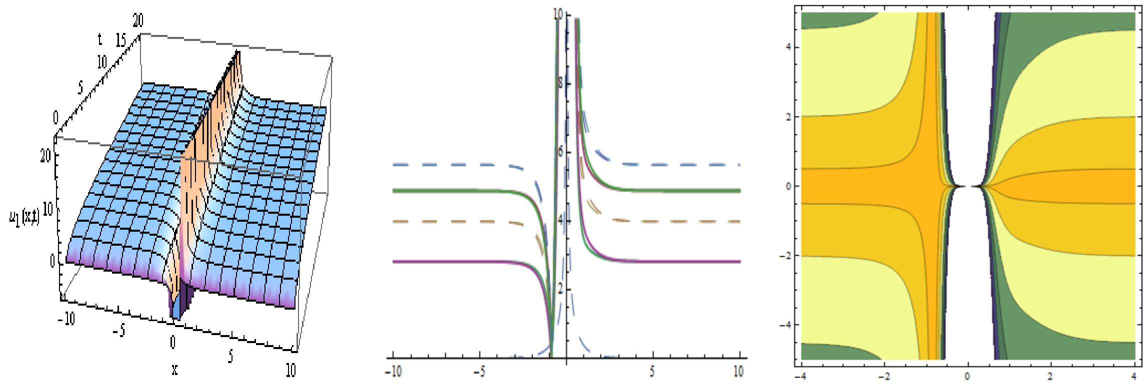

(a) (b) (c)

Figure 2.15: Graphical representation of $u_1(x,t)$ in Eq. (2.4.29) at $\alpha = \frac{1}{2}$ (a) shows 3-D graph x $\in$ [-10, 10] and t $\in$ [0, 5], (b) express 2-D plot in [-10, 10] and [0, 1.0], (c) express contour plot in [-4, 4] and [-4, 4].

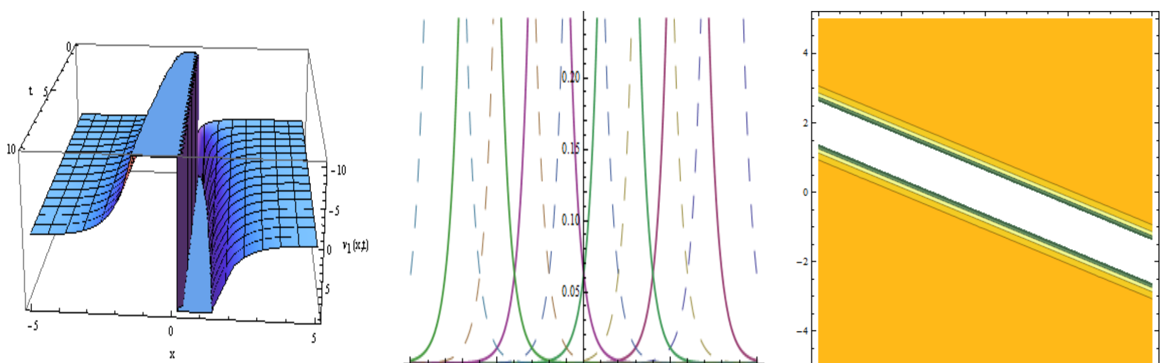

(a) (b) (c)

Figure 2.16: Graphical representation of $v_1(x,t)$ in Eq. (2.4.30) at $\alpha = 1$ (a) shows 3-D graph x $\in$ [-10, 10] and t $\in$ [0, 5], (b) express 2-D plot in [-10, 10] and [0, 1.0], (c) express contour plot in [-4, 4] and [-4, 4].

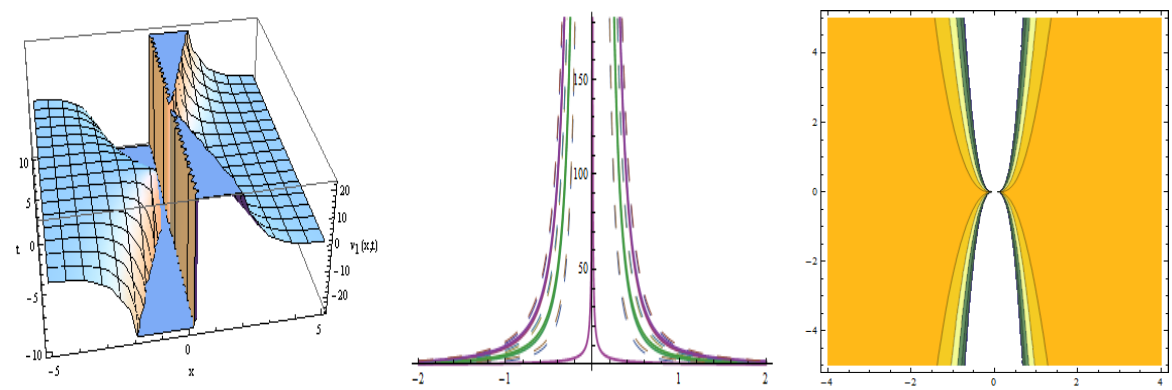

(a) (b) (c)

Figure 2.17: Graphical representation of $v_1(x,t)$ in Eq. (2.4.30) at $\alpha = 2$ (a) shows 3-D graph x $\in$ [-10, 10] and t $\in$ [0, 5], (b) express 2-D plot in [-10, 10] and [0, 1.0], (c) express contour plot in [-4, 4] and [-4, 4].

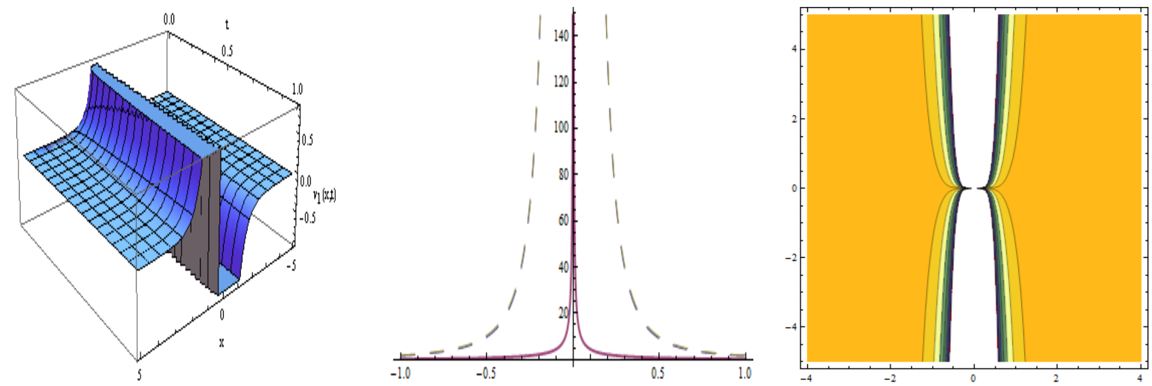

(a) (b) (c)

Figure 2.18: Graphical representation of $v_1(x,t)$ in Eq. (2.4.30) at $\alpha = \frac{1}{2}$ (a) shows 3-D graph x $\in$ [-10, 10] and t $\in$ [0, 5], (b) express 2-D plot in [-10, 10] and [0, 1.0], (c) express contour plot in [-4, 4] and [-4, 4].

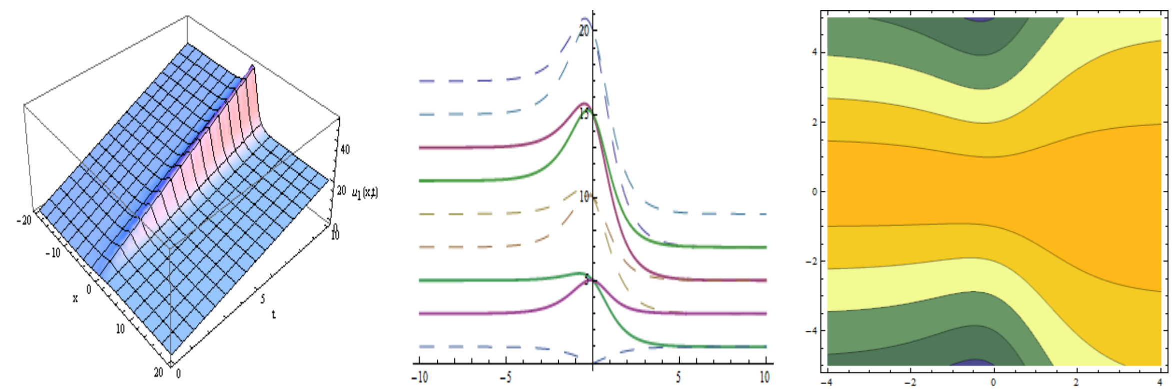

(a) (b) (c)

Figure 2.19: Graphical representation of $u_1(x,t)$ in Eq. (2.4.35) at $\alpha = 1$ (a) shows 3-D graph x $\in$ [-10, 10] and t $\in$ [0, 5], (b) express 2-D plot in [-10, 10] and [0, 1.0], (c) express contour plot in [-4, 4] and [-4, 4].

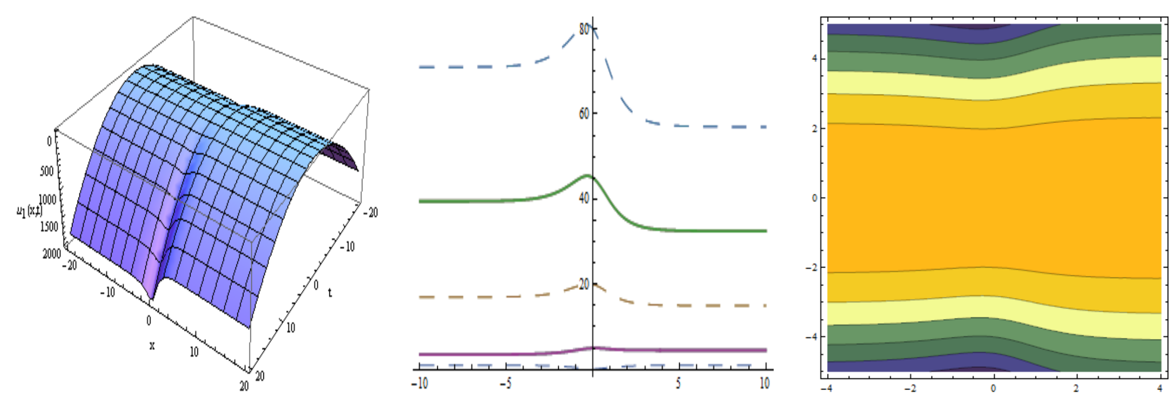

(a) (b) (c)

Figure 2.20: Graphical representation of $u_1(x,t)$ in Eq. (2.4.35) at $\alpha = 2$ (a) shows 3-D graph x $\in$ [-10, 10] and t $\in$ [0, 5], (b) express 2-D plot in [-10, 10] and [0, 1.0], (c) express contour plot in [-4, 4] and [-4, 4].

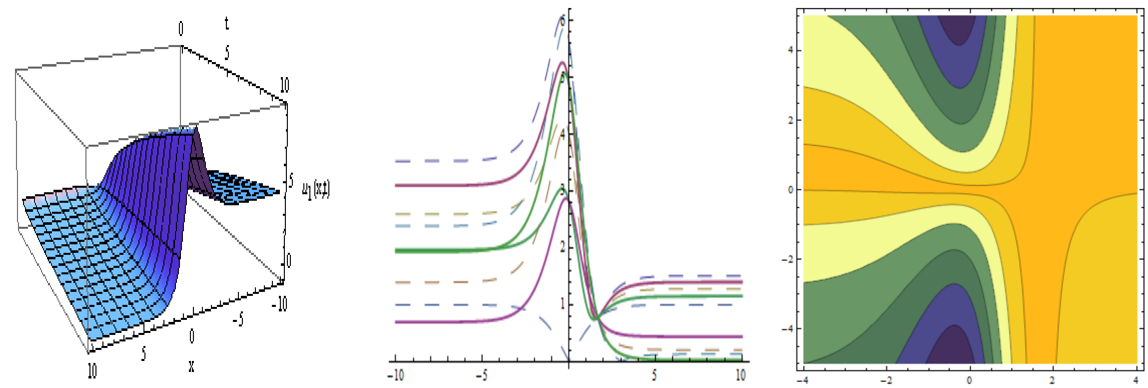

(a) (b) (c)

Figure 2.21: Graphical representation of $u_1(x,t)$ in Eq. (2.4.35) at $\alpha = \frac{1}{2}$ (a) shows 3-D graph x $\in$ [-10, 10] and t $\in$ [0, 5], (b) express 2-D plot in [-10, 10] and [0, 1.0], (c) express contour plot in [-4, 4] and [-4, 4].

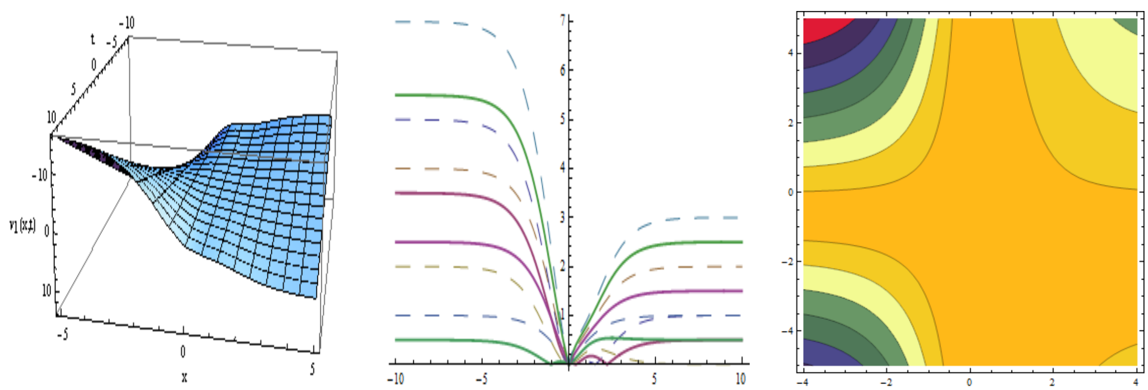

(a) (b) (c)

Figure 2.22: Graphical representation of $v_1(x,t)$ in Eq. (2.4.36) at $\alpha = 1$ (a) shows 3-D graph x $\in$ [-10, 10] and t $\in$ [0, 5], (b) express 2-D plot in [-10, 10] and [0, 1.0], (c) express contour plot in [-4, 4] and [-4, 4].

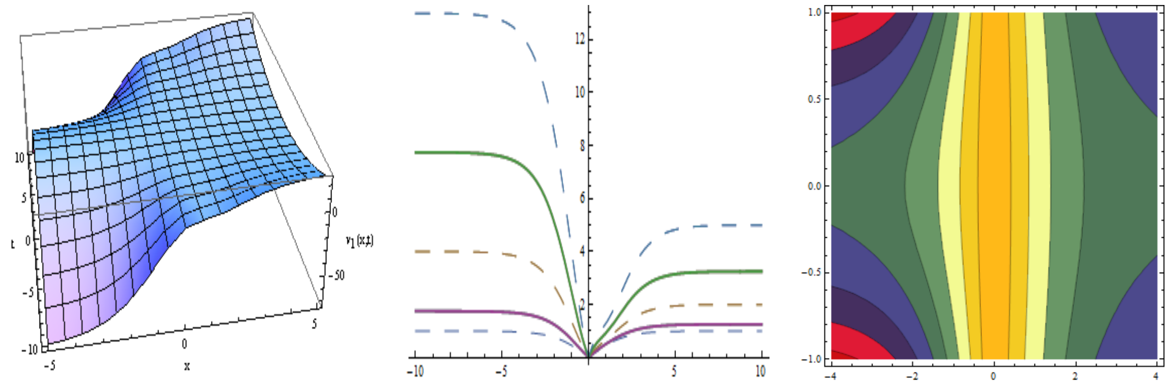

(a) (b) (c)

Figure 2.23: Graphical representation of $v_1(x,t)$ in Eq. (2.4.36) at $\alpha = 2$ (a) shows 3-D graph x $\in$ [-10, 10] and t $\in$ [0, 5], (b) express 2-D plot in [-10, 10] and [0, 1.0], (c) express contour plot in [-4, 4] and [-4, 4].

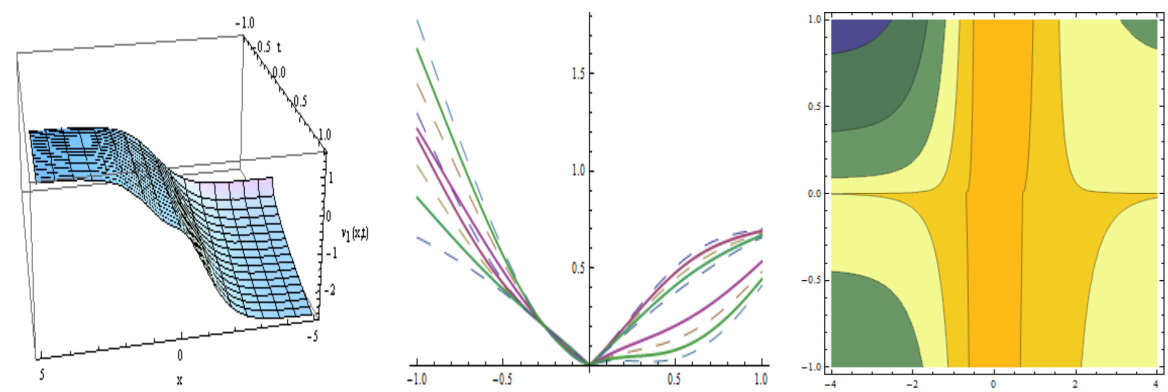

(a) (b) (c)

Figure 2.24: Graphical representation of $v_1(x,t)$ in Eq. (2.4.36) at $\alpha = \frac{1}{2}$ (a) shows 3-D graph x $\in$ [-10, 10] and t $\in$ [0, 5], (b) express 2-D plot in [-10, 10] and [0, 1.0], (c) express contour plot in [-4, 4] and [-4, 4].

Table 2.1: Comparison of exact $u(x,t)$ and approximate solution $u_1(x,t)$

$u(exact)$	$u_1(approximate)$	$Abs\ \ error$
0.882696	0.905261	0.0225654
0.865725	0.979029	0.113304
0.843551	1.07124	0.227689
0.820484	1.16345	0.342966
0.796705	1.25566	0.458955

Table 2.2: Comparison of exact $v(x,t)$ and approximate solution $v_1(x,t)$

$v(exact)$	$v_1(approximate)$	$Abs\ \ error$
0.77239	0.481882	0.290507
0.77239	0.481882	0.290507
0.77239	0.481882	0.290507
0.77239	0.481882	0.290507
0.77239	0.481882	0.290507

The results of this chapter has been published in [44].

Chapter 3

Applications of residual power series and sub ode architectonic to Antagana conformable fractional Lotka-Volterra model

One of the renowned NLPDE is ACFLV model given as [34]:

$$D_t^{\alpha}\Phi = \Phi_{xx} - \beta\Phi + (1+\beta)\Phi^2 - \Phi^3 - \Phi\Psi, \tag{3.0.1}$$

$$D_t^{\alpha}\Psi = \Psi_{xx} + k\Phi\Psi - m\Psi - \delta\Psi^3. \tag{3.0.2}$$

where $0 < \alpha < 1$, k, δ, m, β are positive arbitrary parameters which explains the consumer or predators, biomass of plants, number of prey and mortality rate of predators. x and t describes growth rate of prey and attack time respectively. We suppose the following assumptions for dynamics of the diffusive PP model as $m = \beta$ and $k + \frac{1}{\sqrt{\delta}} - m = 1$. Thus Eq. (3.0.1) and Eq. (3.0.2) becomes

$$D_t^{\alpha}\Phi = \Phi_{xx} - \beta\Phi + (k + \frac{1}{\sqrt{\delta}})\Phi^2 - \Phi^3 - \Phi\Psi, \tag{3.0.3}$$

$$D_t^{\alpha}\Psi = \Psi_{xx} + k\Phi\Psi - \beta\Psi - \delta\Psi^3. \tag{3.0.4}$$

This system is depicted by the population size of predator and prey.

We use following assumption [34],

$$\Phi(x,t) = \Delta(\zeta), \;\; \Psi(x,t) = \Theta(\zeta), \tag{3.0.5}$$

where

$$\zeta = x - \frac{c}{\varepsilon}(t + \frac{1}{\Gamma(\varepsilon)})^{\varepsilon}.$$

Now using Eq. (3.0.5) and its corresponding transformation into Eq. (3.0.3) and Eq. (3.0.4), we get

$$\Delta'' + c\Delta' - \beta\Delta + (k + \frac{1}{\sqrt{\delta}})\Delta^2 - \Delta^3 - \Delta\Theta = 0, \tag{3.0.6}$$

$$\Theta'' + c\Theta' + k\Delta\Theta - \beta\Theta - \delta\Theta^3 = 0. \tag{3.0.7}$$

where c is a constant. By using relation between Δ and Θ as $\Theta = \frac{\Delta}{\sqrt{\delta}}$ yeilds,

$$\Delta'' + c\Delta' - \gamma\Delta + k\Delta^2 - \Delta^3 = 0. \tag{3.0.8}$$

The chapter is written in the following sequence: in sec. 3.1, we use sub-ode approach to obtain bell type solitons, kink and anti-kink type solitons, JEF, WEF, hyperbolic and parabolic functions, in sec. 3.2, we use RPSM to obtain some numerical solutions. In sec. 3.3, we discussed our results in details.

3.1 Sub-ODE method

We will use the following transformation for Eq. (3.0.8) [43]:

$$\Delta(\zeta) = \mu H^r(\zeta), \quad \mu > 0 \tag{3.1.1}$$

where μ is a parameter and $H(\zeta)$ satisfies the equation:

$$H'^2(\zeta) = QH^{2-2p}(\zeta) + RH^{2-p}(\zeta) + SH^2(\zeta) + UH^{2+p}(\zeta) + TH^{2+2p}(\zeta), \; p > 0, \tag{3.1.2}$$

here Q, R, S, T, U are constants. We determine r in Eq. (3.1.1) with the help of homogenous balance technique,

$$D(\zeta) = r, D(\zeta^2) = 2r, , ... \quad D(\zeta') = r + p, D(\zeta'') = r + 2p, ... \tag{3.1.3}$$

we get $p = r$. For Eq. (3.0.8), we get the system of equations:

$$\begin{aligned}
&H^{3p}(\zeta) : 2p^2 T\mu - \mu^3 = 0, \\
&H^{2p}(\zeta) : \frac{3}{2} Tp^2 + U\mu^2 = 0, \\
&H^{p}(\zeta) : m\mu + Sp^2\mu - \gamma\mu = 0,
\end{aligned} \tag{3.1.4}$$

Type 1a. By substituting $Q = R = U = 0$ in Eq. (3.1.4) and we get values of following parameters.

$$\mu = \sqrt{2T}p; \qquad S = \frac{\gamma - m}{p^2},$$

provided that,

$$\Phi_{1,1}(x,t) = \sqrt{2T}p\sqrt{\frac{m-\gamma}{p^2 T}}\,\mathrm{sec}h\left(\frac{p\,\zeta\sqrt{-m+\gamma}}{p}\right), \tag{3.1.5}$$

$$\Psi_{1,1}(x,t) = \frac{1}{\sqrt{\delta}}\sqrt{2T}p\sqrt{\frac{m-\gamma}{p^2 T}}\,\mathrm{sec}h\left(\frac{p\,\zeta\sqrt{-m+\gamma}}{p}\right). \tag{3.1.6}$$

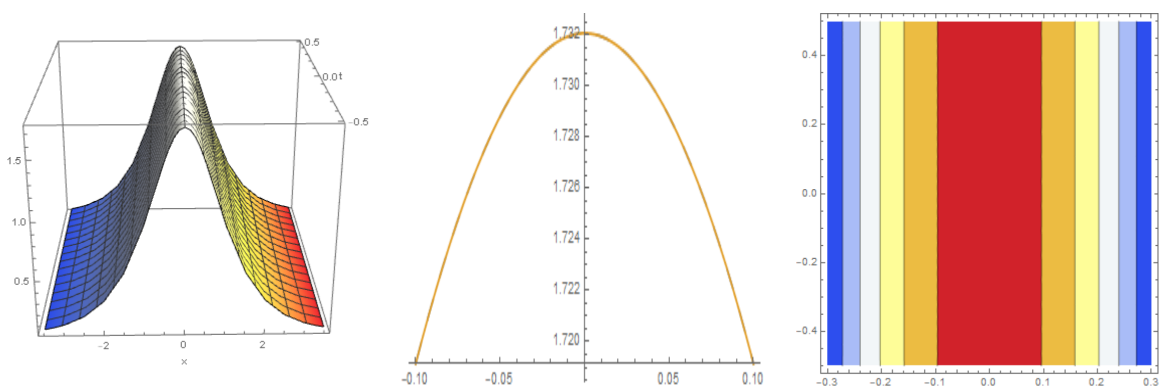

(a) (b) (c)

Figure 3.1: Dynamical behaviour of $\Phi(x,t)$ in Eq. (3.1.5).

Type 1b. By substituting $Q = R = U = 0$ in Eq. (3.1.4) and we get values of following parameters.

$$\mu = \sqrt{2T}p; \qquad S = \frac{\gamma - m}{p^2},$$

provided that

$$\Phi_{1,2}(x,t) = \sqrt{2T}p\sqrt{\frac{m-\gamma}{p^2 T}}\,\sec\left(\frac{p\,\zeta\sqrt{m-\gamma}}{p}\right), \tag{3.1.7}$$

$$\Psi_{1,2}(x,t) = \frac{1}{\sqrt{\delta}}\sqrt{2T}p\sqrt{\frac{m-\gamma}{p^2 T}}\,\sec\left(\frac{p\,\zeta\sqrt{m-\gamma}}{p}\right). \tag{3.1.8}$$

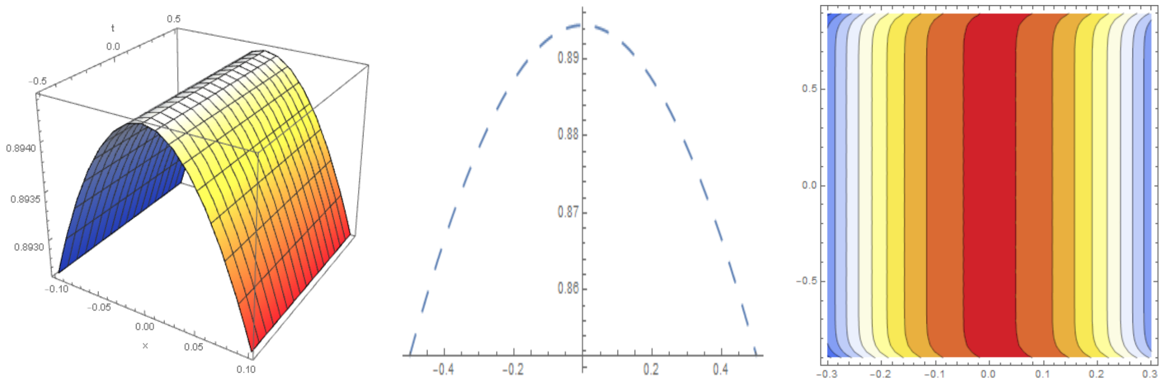

(a) (b) (c)

Figure 3.2: The graph of $\Phi(x,t)$ in Eq. (3.1.7).

Type 1c. By substituting $Q = R = U = 0$ in Eq. (3.1.4) and we get values of following parameters.

$$\mu = \sqrt{2T}p; \qquad S = \frac{\gamma - m}{p^2},$$

provided that

$$\Phi_{1,3}(x,t) = \frac{\sqrt{2}p\varepsilon}{p\zeta}, \tag{3.1.9}$$

$$\Psi_{1,3}(x,t) = \frac{1}{\sqrt{\delta}}\frac{\sqrt{2}p\varepsilon}{p\zeta}. \tag{3.1.10}$$

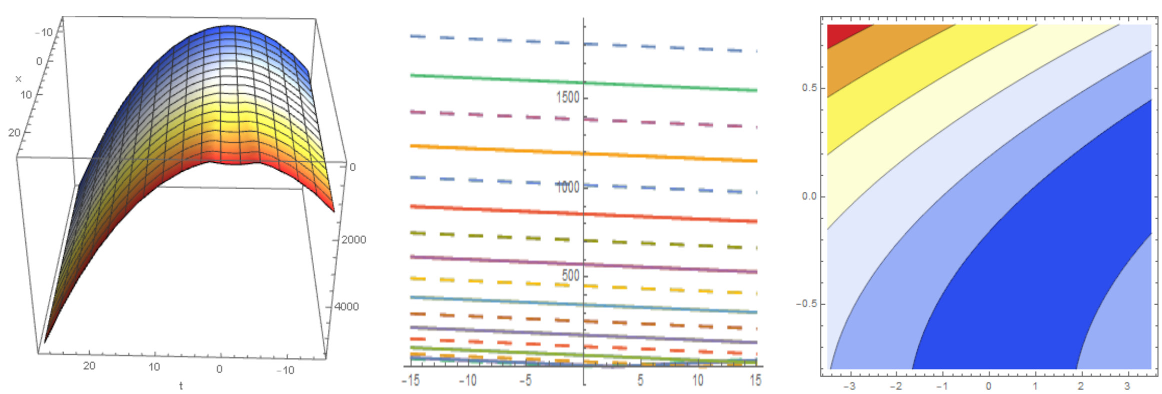

(a) (b) (c)

Figure 3.3: Dynamical behaviour of $\Phi(x,t)$ in Eq. (3.1.9).

Type 2a. By substituting $R = U = 0$ in Eq. Eq. (3.1.4) and we get values of following parameters..

$$\mu = \sqrt{2T}p; \qquad S = \frac{\gamma - m}{p^2},$$

provided that

$$\Phi_{2,1}(x,t) = \sqrt{2T}p\sqrt{\frac{m-\gamma}{p^2T}}\varepsilon \tanh\left(\frac{p\,\zeta\sqrt{m+\gamma}}{p^2}\right), \tag{3.1.11}$$

$$\Psi_{2,1}(x,t) = \frac{1}{\sqrt{\delta}}\sqrt{2T}p\sqrt{\frac{m-\gamma}{p^2T}}\varepsilon \tanh\left(\frac{p\,\zeta\sqrt{m+\gamma}}{p^2}\right). \tag{3.1.12}$$

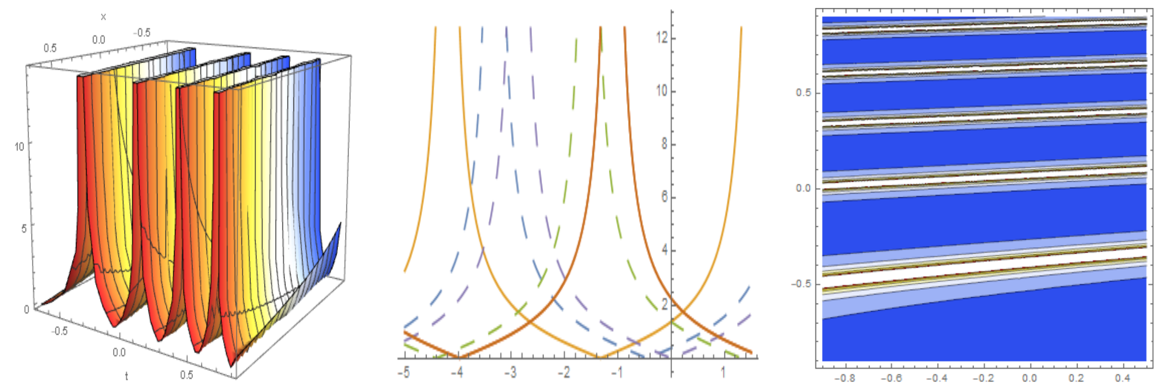

(a) (b) (c)

Figure 3.4: The graphical representation of $\Phi(x,t)$ in Eq. (3.1.11).

Type 2b. By substituting $R = U = 0$ in Eq. (3.1.4) and we get values of following parameters.

$$\mu = \sqrt{2T}p; \qquad S = \frac{\gamma - m}{p^2},$$

provided that

$$\Phi_{2,2}(x,t) = \sqrt{2T}p\sqrt{\frac{m-\gamma}{p^2T}}\varepsilon \tan\left(\frac{p\,\zeta\sqrt{m+\gamma}}{p^2}\right), \tag{3.1.13}$$

$$\Psi_{2,2}(x,t) = \frac{1}{\sqrt{\delta}}\sqrt{2T}p\sqrt{\frac{m-\gamma}{p^2T}}\varepsilon\ \tan\left(\frac{p\,\zeta\sqrt{m+\gamma}}{p^2}\right). \tag{3.1.14}$$

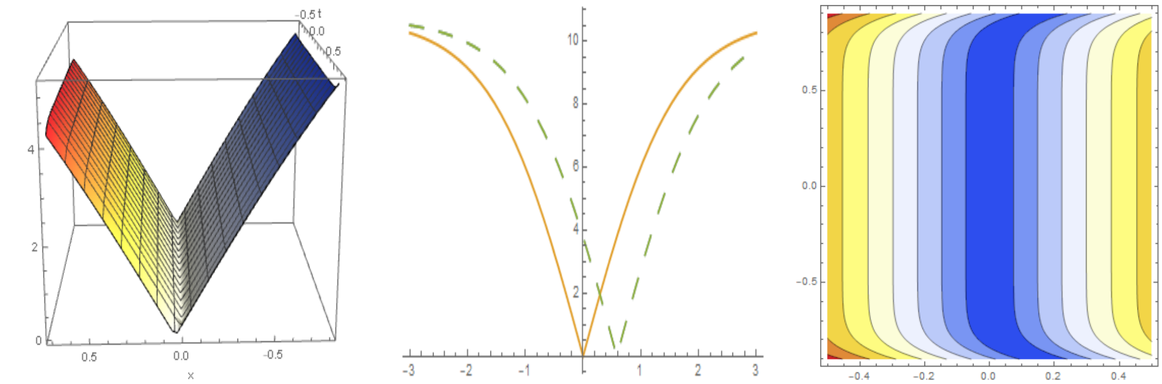

(a) (b) (c)

Figure 3.5: The graph of $\Phi(x,t)$ in Eq. (3.1.13).

Type 3a. By substituting $R = U = 0$ in Eq. (3.1.4) and we get values of following parameters.

$$\mu = \sqrt{2T}\,p; \qquad\qquad S = \frac{\gamma - m}{p^2},$$

provided that,

$$\Phi_{3,1}(x,t) = \sqrt{2T}\,p\sqrt{\frac{m-\gamma}{p^2 T}}\,\sec h\left(\frac{p\,\zeta\sqrt{-m+\gamma}}{p}\right), \tag{3.1.15}$$

$$\Psi_{3,1}(x,t) = \frac{1}{\sqrt{\delta}}\sqrt{2T}\,p\sqrt{\frac{m-\gamma}{p^2 T}}\,\sec h\left(\frac{p\,\zeta\sqrt{-m+\gamma}}{p}\right). \tag{3.1.16}$$

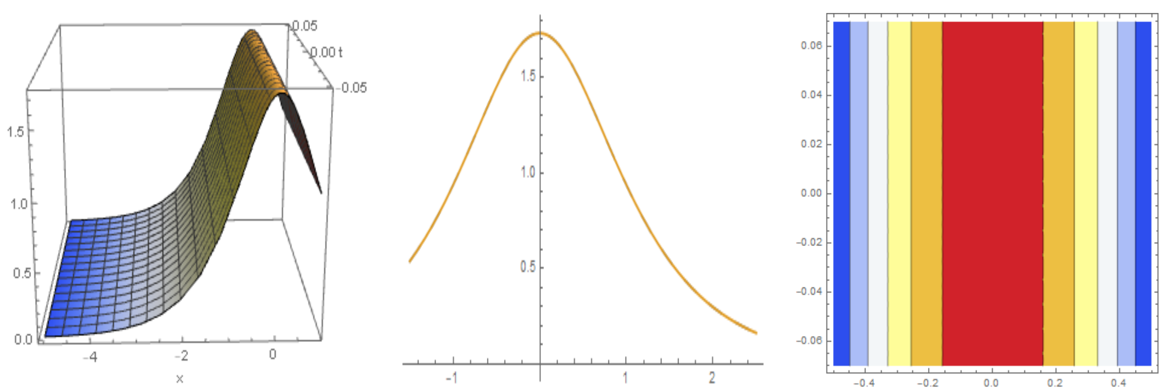

(a) (b) (c)

Figure 3.6: The graph of $\Phi(x,t)$ in Eq. (3.1.15).

Type 3b. By substituting $R = U = 0$ in Eq. (3.1.4) and we get values of following parameters.

$$\mu = \sqrt{2T}p; \qquad S = \frac{\gamma - m}{p^2},$$

provided that

$$\Phi_{3,2}(x,t) = \sqrt{m-\gamma}\operatorname{sec}h\left(\frac{\zeta\sqrt{-m+\gamma}}{\sqrt{2}}\right), \tag{3.1.17}$$

$$\Psi_{3,2}(x,t) = \frac{1}{\sqrt{\delta}}\sqrt{m-\gamma}\operatorname{sec}h\left(\frac{\zeta\sqrt{-m+\gamma}}{\sqrt{2}}\right). \tag{3.1.18}$$

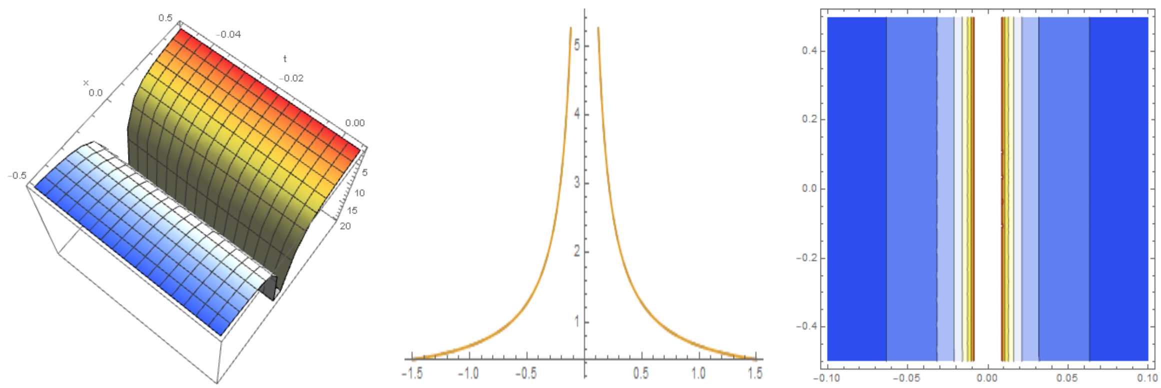

(a) (b) (c)

Figure 3.7: The shape-profile of $\Phi(x,t)$ in Eq. (3.1.17).

Type 4a. By substituting $R = U = 0$ in Eq. (3.1.4) and we get values of following parameters.

$$\mu = \sqrt{2T}p; \qquad S = \frac{\gamma - m}{p^2},$$

provided that

$$\Phi_{4,1}(x,t) = \sqrt{2T}p\sqrt{\frac{m-\gamma}{3p^2} + \wp\left(p\zeta, \frac{4(m-\gamma)^2}{3p^4}, \frac{8(m-\gamma^3)}{27p^6}\right)}, \tag{3.1.19}$$

$$\Psi_{4,1}(x,t) = \frac{1}{\sqrt{\delta}}\sqrt{2T}p\sqrt{\frac{m-\gamma}{3p^2} + \wp\left(p\zeta, \frac{4(m-\gamma)^2}{3p^4}, \frac{8(m-\gamma^3)}{27p^6}\right)}. \tag{3.1.20}$$

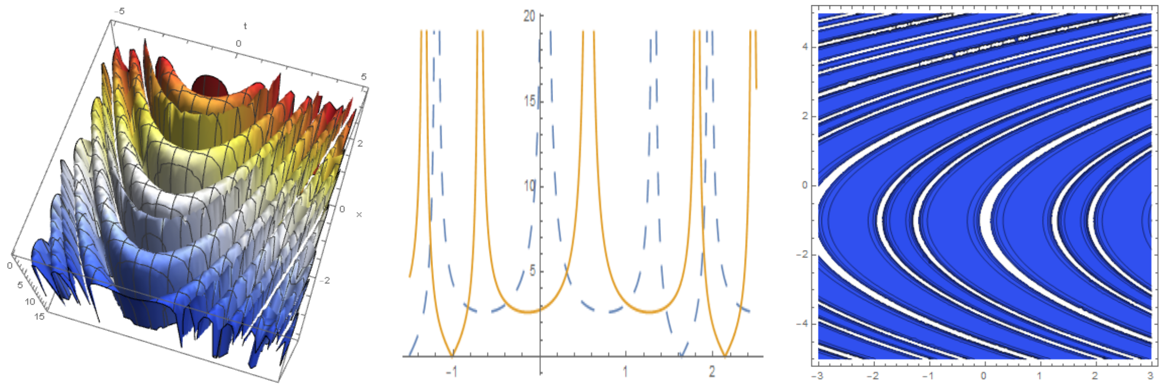

(a) (b) (c)

Figure 3.8: Dynamical behaviour of $\Phi(x,t)$ in Eq. (3.1.19).

Type 4b. By substituting $R = U = 0$ in Eq. (3.1.4) and we get values of following parameters.

$$\mu = \sqrt{2T}p; \qquad S = \frac{\gamma - m}{p^2},$$

provided that

$$\Phi_{4,2}(x,t) = \frac{3\sqrt{2}p^2 p\sqrt{T}\wp\left(p\zeta, \frac{(m-\gamma)^2}{12p^4}, 0\right)}{-m+\gamma+6p^2\wp\left(p\zeta, \frac{(m-\gamma)^2}{12p^4}, 0\right)}, \tag{3.1.21}$$

$$\Psi_{4,2}(x,t) = \frac{1}{\sqrt{\delta}}\frac{3\sqrt{2}p^2 p\sqrt{T}\wp\left(p\zeta, \frac{(m-\gamma)^2}{12p^4}, 0\right)}{-m+\gamma+6p^2\wp\left(p\zeta, \frac{(m-\gamma)^2}{12p^4}, 0\right)}. \tag{3.1.22}$$

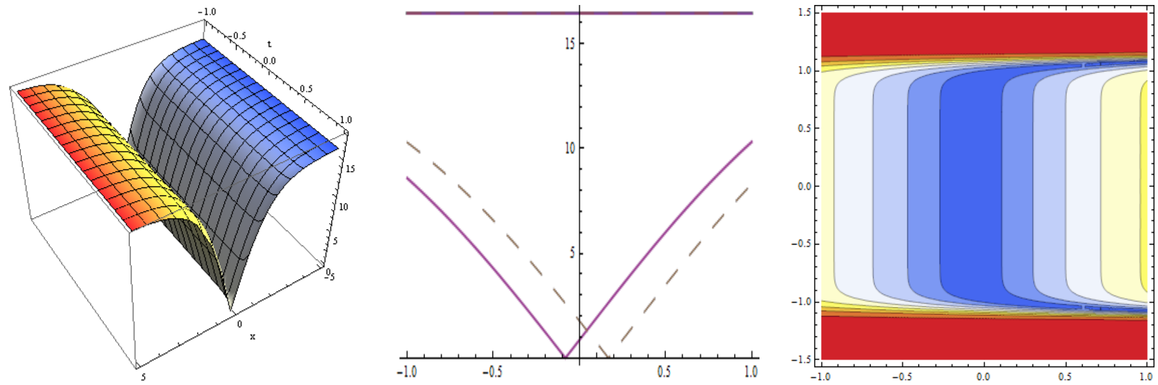

(a) (b) (c)

Figure 3.9: Graphical representation of $\Phi(x,t)$ in Eq. (3.1.21).

Type 5. By substituting $R = U = 0$ in Eq. (3.1.4) and we get values of following parameters.

$$\mu = \sqrt{2T}p; \qquad S = \frac{\gamma - m}{p^2},$$

provided that

$$\Phi_5(x,t) = \frac{\sqrt{15}p^2pT^{\frac{3}{2}}\wp\left(p\zeta, \frac{2(m-\gamma)^2}{9p^4}, \frac{(-m+\gamma)^3}{54p^6}\right)}{m - \gamma - 3p^2\wp\left(p\zeta, \frac{2(m-\gamma)^2}{9p^4}, \frac{(-m+\gamma)^3}{54p^6}\right)}, \tag{3.1.23}$$

$$\Psi_5(x,t) = \frac{1}{\sqrt{\delta}}\frac{\sqrt{15}p^2pT^{\frac{3}{2}}\wp\left(p\zeta, \frac{2(m-\gamma)^2}{9p^4}, \frac{(-m+\gamma)^3}{54p^6}\right)}{m - \gamma - 3p^2\wp\left(p\zeta, \frac{2(m-\gamma)^2}{9p^4}, \frac{(-m+\gamma)^3}{54p^6}\right)}. \tag{3.1.24}$$

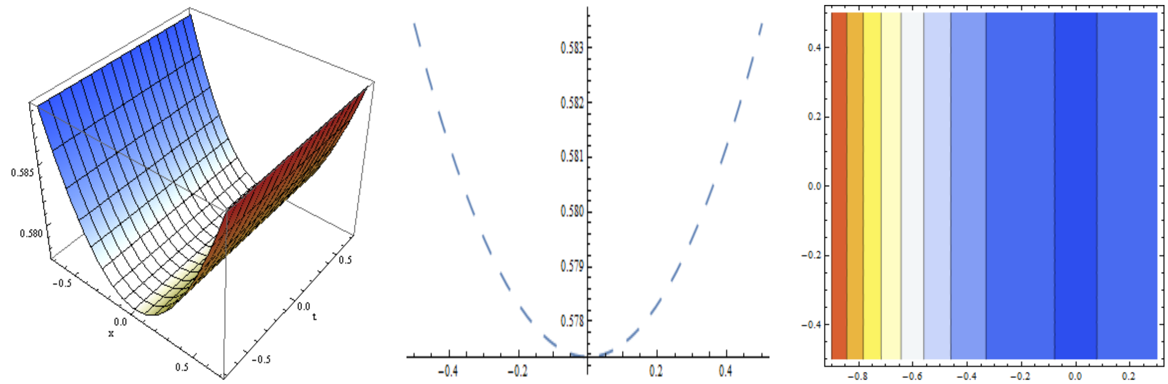

(a) (b) (c)

Figure 3.10: The graph of $\Phi(x,t)$ in Eq. (3.1.23).

Type 6a. By substituting $R = U = 0$ in Eq. (3.1.4) and we get values of following parameters.

$$\mu = \sqrt{2T}p; \qquad S = \frac{\gamma - m}{p^2},$$

provided that

$$\Phi_{6,1}(x,t) = \frac{1}{\frac{n}{3(-m+\gamma)} + \frac{\cosh\left(\frac{p\zeta\sqrt{-m+\gamma}}{p}\right)}{\sqrt{2T}p}}, \tag{3.1.25}$$

$$\Psi_{6,1}(x,t) = \frac{1}{\sqrt{\delta}} \frac{1}{\frac{n}{3(-m+\gamma)} + \frac{\cosh\left(\frac{p\zeta\sqrt{-m+\gamma}}{p}\right)}{\sqrt{2T}p}}. \tag{3.1.26}$$

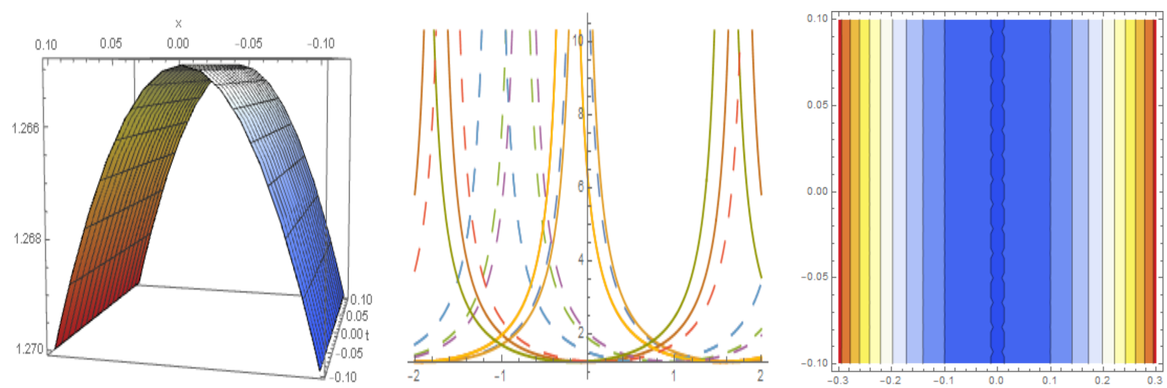

(a) (b) (c)

Figure 3.11: The graphical representation of $\Phi(x,t)$ in Eq. (3.1.25).

Type 6b. By substituting $R = U = 0$ in Eq. (3.1.4) and we get values of following parameters.

$$\mu = \sqrt{2T}\,p; \qquad S = \frac{\gamma - m}{p^2},$$

provided that

$$\Phi_{6,2}(x,t) = \frac{p\sqrt{T}\sqrt{\frac{-m+\gamma}{p^2 T}}\left(1 + \varepsilon \tanh\left(\frac{1}{2} p \zeta \sqrt{\frac{-m+\gamma}{p^2}}\right)\right)}{\sqrt{2}}, \tag{3.1.27}$$

$$\Psi_{6,2}(x,t) = \frac{1}{\sqrt{\delta}} \frac{p\sqrt{T}\sqrt{\frac{-m+\gamma}{p^2 T}}\left(1 + \varepsilon \tanh\left(\frac{1}{2} p \zeta \sqrt{\frac{-m+\gamma}{p^2}}\right)\right)}{\sqrt{2}}. \tag{3.1.28}$$

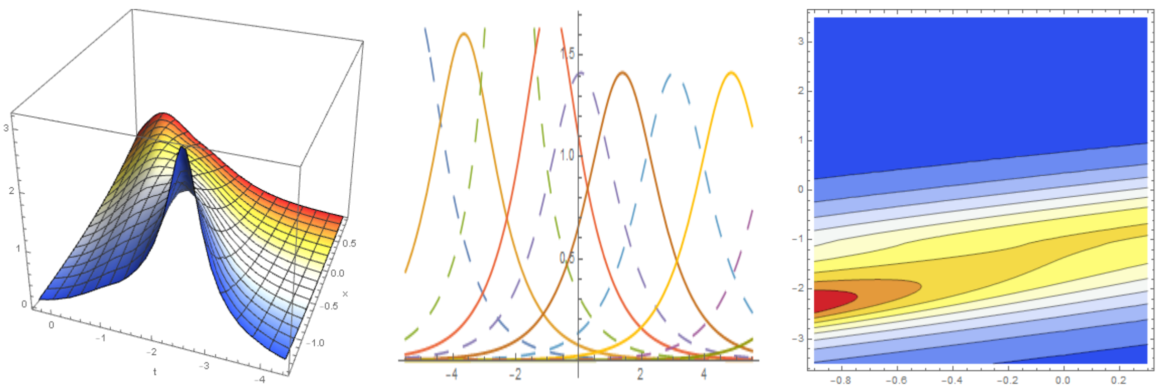

(a) (b) (c)

Figure 3.12: The graph of $\Phi(x,t)$ in Eq. (3.1.27).

Type 6c. By substituting $R = U = 0$ in Eq. (3.1.4) and we get values of following parameters.

$$\mu = \sqrt{2T}\,p; \qquad S = \frac{\gamma - m}{p^2},$$

provided that

$$\Phi_{6,3}(x,t) = \frac{4p\sqrt{2T}}{p\zeta^2 - 4T}, \tag{3.1.29}$$

$$\Psi_{6,3}(x,t) = \frac{1}{\sqrt{\delta}} \frac{4p\sqrt{2T}}{p\zeta^2 - 4T}. \tag{3.1.30}$$

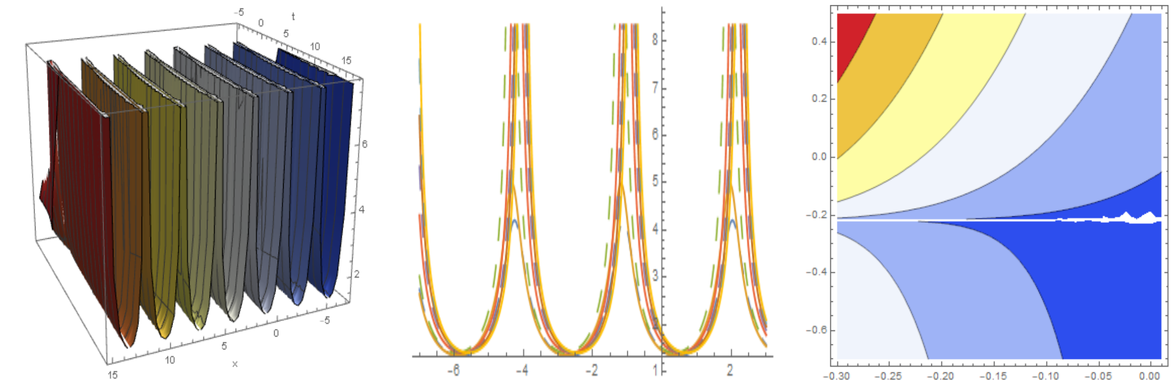

(a) (b) (c)

Figure 3.13: Dynamical behaviour of $\Phi(x,t)$ in Eq. (3.1.29).

Type 7a. By substituting $R = U = 0$ in Eq. (3.1.4) and we get values of following parameters.

$$\mu = \sqrt{2T}\,p; \qquad S = \frac{\gamma - m}{p^2},$$

provided that

$$\Phi_{7,1}(x,t) = \frac{\sqrt{2}p\sqrt{\frac{T(m-\gamma)}{p^2}}\,\sec h^2\left(\frac{1}{2}p\zeta\sqrt{\frac{-m+\gamma}{p^2}}\right)}{\sqrt{T}\left(2-\sec h^2\left(\frac{1}{2}p\zeta\sqrt{\frac{-m+\gamma}{p^2}}\right)\right)}, \tag{3.1.31}$$

$$\Psi_{7,1}(x,t) = \frac{1}{\sqrt{\delta}}\frac{\sqrt{2}p\sqrt{\frac{T(m-\gamma)}{p^2}}\,\sec h^2\left(\frac{1}{2}p\zeta\sqrt{\frac{-m+\gamma}{p^2}}\right)}{\sqrt{T}\left(2-\sec h^2\left(\frac{1}{2}p\zeta\sqrt{\frac{-m+\gamma}{p^2}}\right)\right)}. \tag{3.1.32}$$

Type 7b. By substituting $R = U = 0$ in Eq. (3.1.4) and we get values of following parameters.

$$\mu = \sqrt{2T}\,p; \qquad S = \frac{\gamma - m}{p^2},$$

provided that

$$\Phi_{7,2}(x,t) = -\frac{\sqrt{2}p\sqrt{\frac{T(m-\gamma)}{p^2}}\,\csc h^2\left(\frac{1}{2}p\zeta\sqrt{\frac{-m+\gamma}{p^2}}\right)}{\sqrt{T}\left(2+\csc h^2\left(\frac{1}{2}p\zeta\sqrt{\frac{-m+\gamma}{p^2}}\right)\right)}, \tag{3.1.33}$$

$$\Psi_{7,2}(x,t) = -\frac{1}{\sqrt{\delta}} \frac{\sqrt{2}p\sqrt{\frac{T(m-\gamma)}{p^2}}\operatorname{csc}h^2\left(\frac{1}{2}p\zeta\sqrt{\frac{-m+\gamma}{p^2}}\right)}{\sqrt{T}\left(2+\operatorname{csc}h^2\left(\frac{1}{2}p\zeta\sqrt{\frac{-m+\gamma}{p^2}}\right)\right)}. \tag{3.1.34}$$

Type 8a. By substituting $R = U = 0$ in Eq. (3.1.4) and we get values of following parameters.

$$\mu = \sqrt{2T}p; \qquad S = \frac{\gamma - m}{p^2},$$

provided that

$$\Phi_{8,1}(x,t) = \frac{\sqrt{2}p\sqrt{\frac{T(m-\gamma)}{p^2}}\sec^2\left(\frac{1}{2}p\zeta\sqrt{\frac{-m+\gamma}{p^2}}\right)}{\sqrt{T}\left(2-\sec^2\left(\frac{1}{2}p\zeta\sqrt{\frac{-m+\gamma}{p^2}}\right)\right)}, \tag{3.1.35}$$

$$\Psi_{8,1}(x,t) = \frac{1}{\sqrt{\delta}} \frac{\sqrt{2}p\sqrt{\frac{T(m-\gamma)}{p^2}}\sec^2\left(\frac{1}{2}p\zeta\sqrt{\frac{-m+\gamma}{p^2}}\right)}{\sqrt{T}\left(2-\sec^2\left(\frac{1}{2}p\zeta\sqrt{\frac{-m+\gamma}{p^2}}\right)\right)}. \tag{3.1.36}$$

Type 8b. By substituting $R = U = 0$ in Eq. (3.1.4) and we get values of following parameters.

$$\mu = \sqrt{2T}p; \qquad S = \frac{\gamma - m}{p^2},$$

provided that

$$\Phi_{8,2}(x,t) = -\frac{\sqrt{2}p\sqrt{\frac{T(m-\gamma)}{p^2}}\csc^2\left(\frac{1}{2}p\zeta\sqrt{\frac{-m+\gamma}{p^2}}\right)}{\sqrt{T}\left(2-\csc^2\left(\frac{1}{2}p\zeta\sqrt{\frac{-m+\gamma}{p^2}}\right)\right)}, \tag{3.1.37}$$

$$\Psi_{8,2}(x,t) = -\frac{1}{\sqrt{\delta}} \frac{\sqrt{2}p\sqrt{\frac{T(m-\gamma)}{p^2}}\csc^2\left(\frac{1}{2}p\zeta\sqrt{\frac{-m+\gamma}{p^2}}\right)}{\sqrt{T}\left(2-\csc^2\left(\frac{1}{2}p\zeta\sqrt{\frac{-m+\gamma}{p^2}}\right)\right)}. \tag{3.1.38}$$

In the next section, we will find power series solutions using RPSM [23].

3.2 RPSM method [22]

Consider Eq. (3.0.1) and Eq. (3.0.2), subject to the initial conditions.

$$\Phi(x,0) = f_0(x), \tag{3.2.1}$$

$$\Psi(x,0) = g_0(x). \tag{3.2.2}$$

We define a residual function for Eq. (3.0.1) and Eq. (3.0.2) as

$$Res_{\Phi}(x,t) = D_t^{\alpha}\Phi - \Phi_{xx} + \beta\Phi - (1+\beta)\Phi^2 + \Phi^3 + \Phi\Psi, \tag{3.2.3}$$

$$Res_{\Psi}(x,t) = D_t^{\alpha}\Psi - \Psi_{xx} - k\Phi\Psi + m\Psi + \delta\Psi^3. \tag{3.2.4}$$

Therefore the kth residual function $Res_{\Phi,k}(x,t)$ and $Res_{\Psi,k}(x,t)$

$$Res_{\Phi,k}(x,t) = D_t^{\alpha}\Phi_k - \Phi_{k,xx} + \beta\Phi_k - (1+\beta)\Phi_k^2 + \Phi_k^3 + \Phi_k\Psi_k, \tag{3.2.5}$$

$$Res_{\Psi,k}(x,t) = D_t^{\alpha}\Psi_k - \Psi_{k,xx} - k\Phi_k\Psi_k + m\Psi_k + \delta\Psi_k^3. \tag{3.2.6}$$

Let us consider the series solution [22],

$$\Phi_k(x,t) = f_0(x) + \Sigma_{n=1}^{k} f_n(x)\frac{t^{\alpha}}{\Gamma(1+n\alpha)}, \tag{3.2.7}$$

$$\Psi_k(x,t) = g_0(x) + \Sigma_{n=1}^{k} g_n(x)\frac{t^{\alpha}}{\Gamma(1+n\alpha)}. \tag{3.2.8}$$

To find the f_1 and g_1 put $k=1$, then

$$\Phi_1(x,t) = f_0(x) + f_1(x)\frac{t^{\alpha}}{\Gamma(1+\alpha)}, \tag{3.2.9}$$

$$\Psi_1(x,t) = g_0(x) + g_1(x)\frac{t^{\alpha}}{\Gamma(1+\alpha)}. \tag{3.2.10}$$

$$Res_{\Phi,1}(x,t) = D_t^{\alpha}\Phi_1 - \Phi_{1,xx} + \beta\Phi_1 - (1+\beta)\Phi_1^2 + \Phi_1^3 + \Phi_1\Psi_1, \tag{3.2.11}$$

$$Res_{\Psi,1}(x,t) = D_t^{\alpha}\Psi_1 - \Psi_{1,xx} - k\Phi_1\Psi_1 + m\Psi_1 + \delta\Psi_1^3. \tag{3.2.12}$$

put Eq. (3.2.9) and Eq. (3.2.10) into Eq. (3.2.11) and Eq. (3.2.11) respectively, then

$$\begin{aligned} Res_{\Phi,1}(x,t) = {} & f_1(x) - (f_0''(x) + f_1''(x)\frac{t^{\alpha}}{\Gamma(1+\alpha)}) + \beta(f_0(x) + f_1(x)\frac{t^{\alpha}}{\Gamma(1+\alpha)}) - (1+\beta)(f_0(x) + f_1(x)\frac{t^{\alpha}}{\Gamma(1+\alpha)} \\ & + (f_0(x) + f_1(x)\frac{t^{\alpha}}{\Gamma(1+\alpha)})^3 + (f_0(x) + f_1(x)\frac{t^{\alpha}}{\Gamma(1+\alpha)})(g_0(x) + g_1(x)\frac{t^{\alpha}}{\Gamma(1+\alpha} \end{aligned}$$

$$\begin{aligned} Res_{\Psi,1}(x,t) = {} & g_1(x) - (g_0''(x) + g_1''(x)\frac{t^{\alpha}}{\Gamma(1+\alpha)}) - k(f_0(x) + f_1(x)\frac{t^{\alpha}}{\Gamma(1+\alpha)})(g_0(x) + g_1(x)\frac{t^{\alpha}}{\Gamma(1+\alpha)}) \\ & + m(g_0(x) + g_1(x)\frac{t^{\alpha}}{\Gamma(1+\alpha)}) + \delta(g_0(x) + g_1(x)\frac{t^{\alpha}}{\Gamma(1+\alpha)})^3. \end{aligned}$$

By given initial condition we have,

$$D_t^{(k-1)\alpha}\Phi_k(x,0) = 0, \tag{3.2.13}$$

$$D_t^{(k-1)\alpha}\Psi_k(x,0) = 0. \tag{3.2.14}$$

$$f_1(x) = f_0''(x) - \beta f_0(x) + (1+\beta)f_0^2(x) + f_0^3(x) + f_0(x)g_0(x), \tag{3.2.15}$$

$$g_1(x) = g_0''(x) + kf_0(x)g_0(x) - mg_0(x) - \delta 1 g_0^3(x). \tag{3.2.16}$$

Similarly, we can find higher order terms by putting $k = 2, 3, 4, \ldots$

Now, Eq. (3.2.9) and Eq. (3.2.10) becomes,

$$\Phi_1(x,t) = f_0(x) + (f_0''(x) - \beta f_0(x) + (1+\beta) f_0^2(x) + f_0^3(x) + f_0(x) g_0(x)) \frac{t^\alpha}{\Gamma(1+\alpha)}, \quad (3.2.17)$$

$$\Psi_1(x,t) = g_0(x) + (g_0''(x) + k f_0(x) g_0(x) - m g_0(x) - \delta 1 g_0^3(x)) \frac{t^\alpha}{\Gamma(1+\alpha)}. \quad (3.2.18)$$

Case 1:

$$\Phi(x,0) = f_0(x) = \lambda \sec h(\sqrt{\frac{\lambda^2(c-1)}{2}}(x)), \quad (3.2.19)$$

$$\Psi(x,0) = g_0(x) = \gamma \sec h(\sqrt{\frac{\lambda^2(c-1)}{2}}(x)). \quad (3.2.20)$$

Now replacing the values of $f_0(x)$ and $g_0(x)$ in Eq. (3.2.17) and Eq. (3.2.18),

$$\Phi_1(x,t) = \lambda \sec h\left(\sqrt{\frac{\lambda^2(c-1)}{2}}(x)\right) + \left(5\beta - \frac{8\gamma\lambda}{1 + 2\lambda^2 + \cosh(\lambda\sqrt{2-2c}x)} - \lambda \sec h\left(\sqrt{\frac{\lambda^2(c-1)}{2}}(x\right.\right.$$
$$+\frac{1}{2}(c-1)\lambda^3 \sec h(\sqrt{\frac{\lambda^2(c-1)}{2}}(x)) - 4(c-1)\lambda^3 \operatorname{csc} h^3\left(\sqrt{\frac{\lambda^2(c-1)}{2}}(x)\right) \sinh^5\left(\sqrt{\frac{\lambda^2(c-1)}{2}}(x)\right)\bigg)\frac{t^\alpha}{\Gamma(1+\alpha}$$

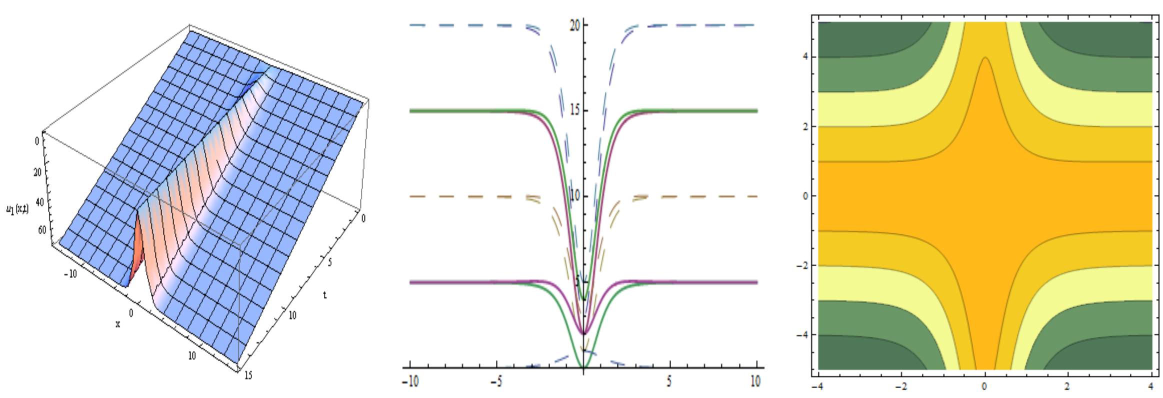

(a) (b) (c)

Figure 3.14: The Dynamical behaviour of $\Phi_1(x,t)$ in Eq. (3.2.21).

$$\Psi_1(x,t) = \left(\gamma + \frac{m\lambda}{2}(2+\gamma\lambda(c-1) - \frac{4\gamma\cosh\left(\sqrt{\frac{\lambda^2(c-1)}{2}}(x)\right)}{1+2\lambda^2+\cosh(\lambda\sqrt{2-2cx})})\sec h\left(\sqrt{\frac{\lambda^2(c-1)}{2}}(x)\right)\right)\frac{t^\alpha}{\Gamma(1+\alpha)} \quad (3.2.22)$$

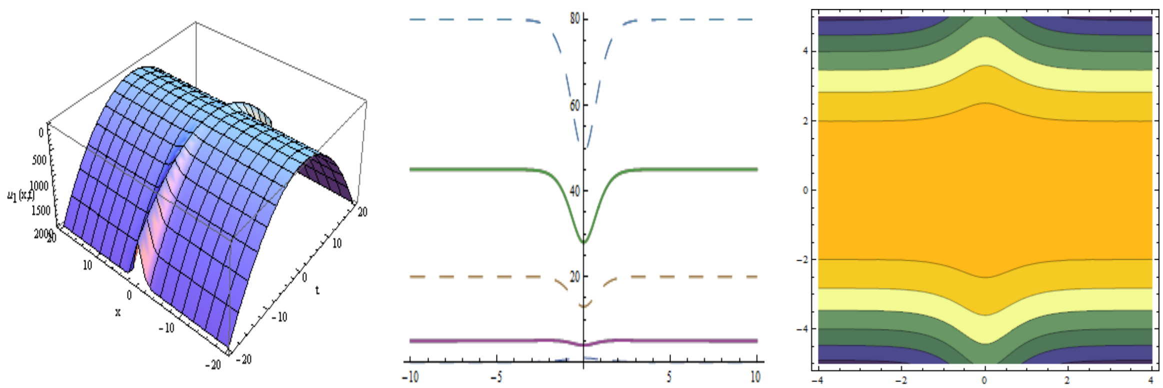

(a) (b) (c)

Figure 3.15: The graph of $\Psi_1(x,t)$ in Eq. (3.2.22).

Case 2:

$$\Phi(x,0) = f_0(x) = A\text{ş}ch(\sqrt{c-1}(x)), \quad (3.2.23)$$

$$\Psi(x,0) = g_0(x) = B\operatorname{csc}h(\sqrt{c-1}(x)). \quad (3.2.24)$$

Now replacing the values of $f_0(x)$ and $g_0(x)$ in Eq. (3.2.17) and Eq. (3.2.18),

$$\begin{aligned}\Phi_1(x,t) = A(\operatorname{csc}h(\sqrt{1-c})x) + \Bigg(&5\beta - A\operatorname{csc}h(\sqrt{1-c}x) - (-1+c)A\coth(\sqrt{1-c}x)^2\operatorname{csc}h(\sqrt{1-c}x)\\ &-(-1+c)A\operatorname{csc}h(\sqrt{1-c}x)^3 - \frac{4AB\operatorname{csc}h(\sqrt{1-c}x)^2}{1+A^2\operatorname{csc}h(\sqrt{1-c}x)^2}\Bigg)\frac{t^\alpha}{\Gamma(1+\alpha)} \quad (3.2.25)\end{aligned}$$

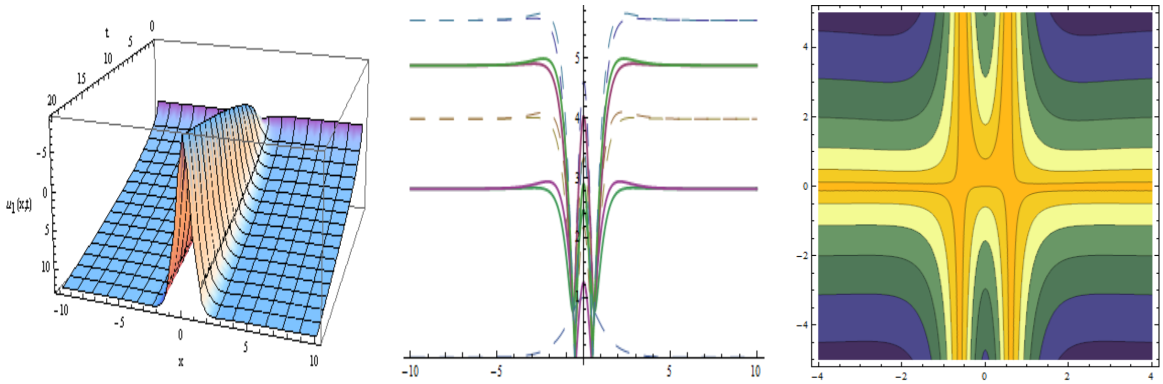

(a) (b) (c)

Figure 3.16: Graphical representation of $\Phi_1(x,t)$ in Eq. (3.2.25) at $\alpha = \frac{1}{2}$.

$$\Psi_1(x,t) = B\csc h(\sqrt{1-cx}) + \Bigg(A\csc h(\sqrt{1-cx}) - (-1+c)B\coth(\sqrt{1-cx})^2\csc h(\sqrt{1-cx}) - (-1+c)B\csc h(\sqrt{1-cx})^3 - \frac{AB\csc h(\sqrt{1-cx})^2}{1+A^2\csc h(\sqrt{1-cx})^2}\Bigg)\frac{t^\alpha}{\Gamma(1+\alpha)} \tag{3.2.26}$$

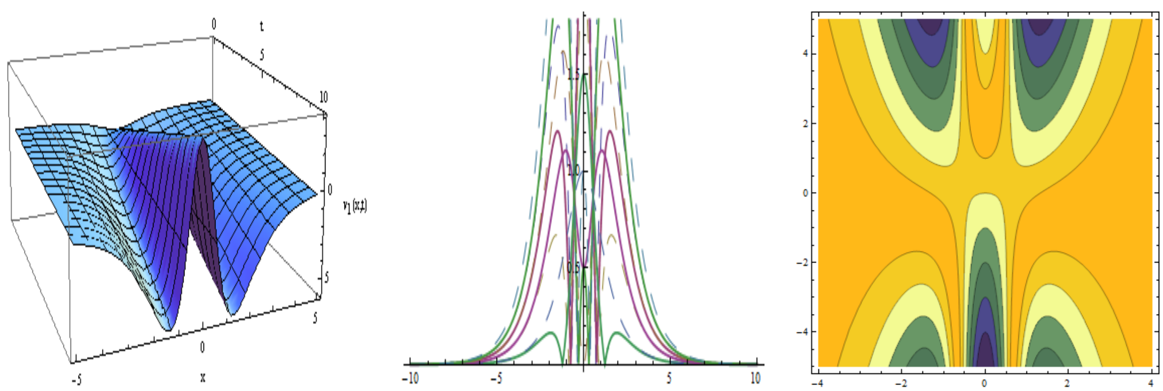

(a) (b) (c)

Figure 3.17: Dynamical behaviour of $\Psi_1(x,t)$ in Eq. (3.2.26).

Case 3:

$$\Phi(x,0) = f_0(x) = \lambda\tanh^2(\sqrt{\frac{(c-1)}{8}}(x)), \tag{3.2.27}$$

$$\Psi(x,0) = g_0(x) = \gamma \tanh^4(\sqrt{\frac{(c-1)}{8}}(x)). \tag{3.2.28}$$

Now replacing the values of $f_0(x)$ and $g_0(x)$ in Eq. (3.2.17) and Eq. (3.2.18),

$$\Phi_1(x,t) = \lambda \tanh\left(\frac{(\sqrt{1-cx})}{(2\sqrt{2})}\right) + \left(5\beta + 2(-1+c)\lambda \operatorname{csc}h(\sqrt{1-cx})\sqrt{2}^3 \sinh\frac{(\sqrt{1-cx})^4}{(2\sqrt{2})} - \right.$$
$$\left. -\lambda \tanh\left(\frac{\sqrt{1-cx}}{2\sqrt{2}}\right) - \frac{4\lambda\gamma \tanh^2\left(\frac{\sqrt{1-cx}}{2\sqrt{2}}\right)}{1+\lambda^2 \tanh^2\left(\frac{(\sqrt{1-cx})}{2\sqrt{2}}\right)}\right)\frac{t^\alpha}{\Gamma(1+\alpha)} \tag{3.2.29}$$

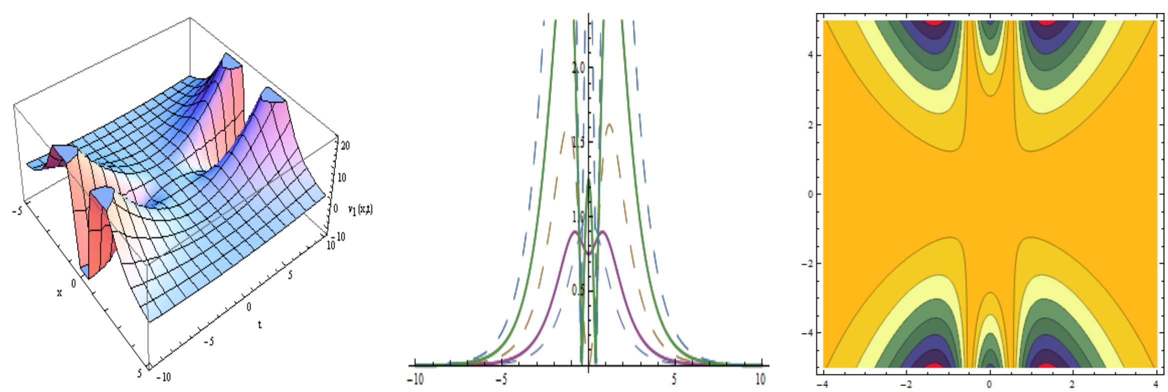

(a) (b) (c)

Figure 3.18: Dynamical behaviour of $\Phi_1(x,t)$ in Eq. (3.2.29) at $\alpha = 2$.

$$\Psi_1(x,t) = \gamma \tanh\left(\frac{(\sqrt{1-cx})}{(2\sqrt{2})}\right) + \left(2(-1+c)\gamma \operatorname{csc}h^3\left(\frac{(\sqrt{1-cx})}{2\sqrt{2}}\right)\sinh^4\left(\frac{(\sqrt{1-cx})}{(2\sqrt{2})}\right) + \right.$$
$$\left. +\lambda \tanh\left(\frac{(\sqrt{1-cx})}{(2\sqrt{2})}\right) - \frac{\gamma\lambda \tanh^2\left(\frac{\sqrt{1-cx}}{2\sqrt{2}}\right)}{(1+\lambda^2 \tanh^2\left(\frac{(\sqrt{1-cx})}{(\sqrt{2})}\right))}\right)\frac{t^\alpha}{\Gamma(1+\alpha)} \tag{3.2.30}$$

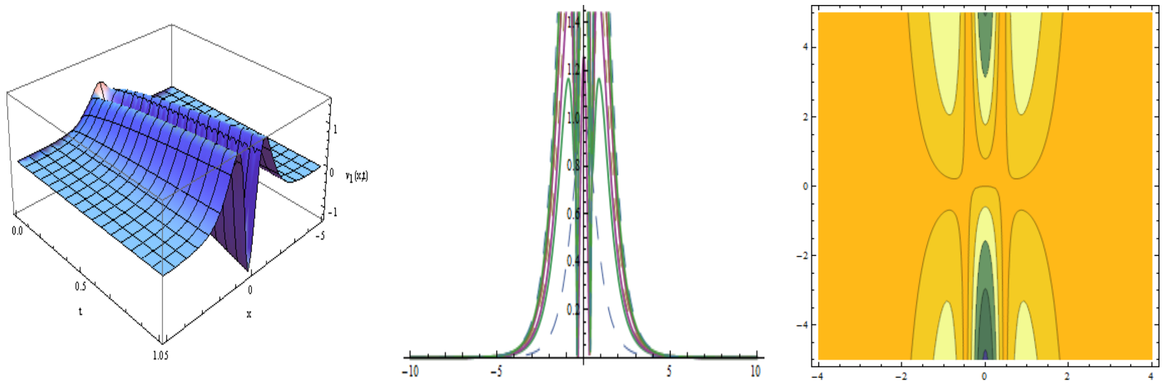

(a) (b) (c)

Figure 3.19: Graphical representation of $\Psi_1(x,t)$ in Eq. (3.2.30) at $\alpha = \frac{1}{2}$.

Case 4:

$$\Phi(x,0) = f_0(x) = \sqrt{\frac{2(m-\gamma)}{p^2}}p\sec\left(p\sqrt{\frac{(\gamma-m)}{p}}(x)\right), \tag{3.2.31}$$

$$\Psi(x,0) = g_0(x) = \sqrt{\frac{2(m-\gamma)}{p^2\delta}}p\sec\left(p\sqrt{\frac{(\gamma-m)}{p}}(x)\right). \tag{3.2.32}$$

Now replacing the values of $f_0(x)$ and $g_0(x)$ in Eq. (3.2.17) and Eq. (3.2.18),

$$\Phi_1(x,t) = \sqrt{2p}\sqrt{\frac{m-\gamma}{p^2}}\sec(\sqrt{m-\gamma x}) + \Bigg(-5\beta - \sqrt{2}\sqrt{p}\sqrt{\frac{m-\gamma}{p^2}}\sec(x\sqrt{m-\gamma}) + \sqrt{2}p^{5/2}((m-\gamma)/p^2)^{3/2}\,\mathrm{se}$$

$$-(8m\sqrt{p/\delta}\sec^2(x\sqrt{m-\gamma}))p^{3/2}(1+(2(m-\gamma)\sec^2(x\sqrt{m-\gamma})p + \frac{8\gamma\sqrt{\frac{p}{\delta}}\sec(x\surd}{p^{3/2}(1+(2(m-\gamma)\,\mathrm{sec}}$$

$$+\sqrt{2}p^{5/2}(\frac{(m-\gamma)}{p^2})^{3/2}\sec(x\sqrt{m-\gamma})\tan^2(x\sqrt{m-}$$

$$
\begin{aligned}
\Psi_1(x,t) = \sqrt{\frac{2p}{\delta}}\sqrt{\frac{(m-\gamma)}{p^2}}\sec(\sqrt{m-\gamma}x) + \sqrt{2}\sqrt{p}\sqrt{\frac{(m-\gamma)}{p^2}}\sec(x\sqrt{m-\gamma}) + \Bigg(\sqrt{2}p(\frac{m-\gamma}{p^2})^{3/2}(\frac{p}{\delta})^{3/2}\delta\sec^3(\\
-\frac{2m\sqrt{\frac{p}{\delta}}\sec^2(x\sqrt{m-\gamma^2})}{p^{3/2}(1+\frac{(2(m-\gamma)\sec^2\sqrt{m-\gamma})}{p})} + \frac{(2\gamma\sqrt{\frac{p}{\delta}}\sec^2(x\sqrt{}}{p^{3/2}(\frac{1+(2(m-\gamma)\sec^2}{p}}\\
+\sqrt{2}p(\frac{(m-\gamma)}{p^2})^{3/2}(\frac{p}{\delta})^{3/2}\delta\sec(x\sqrt{m-\gamma})\tan^2(x\sqrt{m-\gamma})\Bigg)
\end{aligned}
$$

Table 3.1: Comparison of exact $\Phi(x,t)$ and approximate solution $\Phi_1(x,t)$

$\Phi(exact)$	$\Phi_1(approximate)$	$Abs\ \ error$
0.882696	0.905261	0.0225654
0.865725	0.979029	0.113304
0.843551	1.07124	0.227689
0.820484	1.16345	0.342966
0.796705	1.25566	0.458955

Table 3.2: Comparison of exact $\Psi(x,t)$ and approximate solution $\Psi_1(x,t)$

$\Psi(exact)$	$\Psi_1(approximate)$	$Abs\ \ error$
0.77239	0.481882	0.290507
0.77239	0.481882	0.290507
0.77239	0.481882	0.290507
0.77239	0.481882	0.290507
0.77239	0.481882	0.290507

3.3 Results and Discussion

This model was solved by extended simplest equation method, modified Kudryashov technique, cubic B-spline scheme and also compare numerical results [34]. Khalighi et al. worked on stability of this model using Caputo and Caputo-Fabrizo derivative [36]. In this manuscript, we find exact and numerical solutions for this model with aid of various techniques, namely sub-ode method and RPSM. Sub-ode method gives the analytic solutions like bell type, kink type, anti-kink type solitons, JEF, WEF, hyperbolic function, parabolic function. RPSM is applied to obtain power series solution. We also classified the structure of our new achieved solutions, and also shown graphs in 3-D, 2-D and contour shapes. Fig. a shows 3-D, Fig. b shows 2-D and Fig. c shows contour by using different values.

Fig. (3.1) and Fig. (3.2) shows bell type solitons, Fig. (3.3) shows bell type solitons, Fig. (3.4) and Fig. (3.5) shows kink type solitons, Fig. (3.6) and Fig. (3.7) shows bell type solitons, Fig. (3.8) shows JEF, Fig. (3.9) and Fig. (3.10) shows WEF, Fig. (3.11) shows parabolic function, Fig. (3.12) shows anti-kink type solitons, Fig. (3.13) shows parabolic function, Fig. (3.14) and Fig. (3.15) shows bell type solitons, Fig. (3.16) and Fig. (3.17) shows kink and anti-kink type solitons, Fig. (3.18) shows hyperbolic function, Fig. (3.19) shows bell type solitons.

Chapter 4

Conclusion

NLEEs have shown their importance in distinct field of sciences. In this whole work, we studied two different kinds of nonlinear models. The computation of exact and analytical solutions in mathematical physics acts a key role in soliton theory. So, it's very important to trace closed-form and effected soliton solutions for nonlinear models. These solutions provide information about the systematization of the intricate real phenomena. We obtained four types of solutions i.e bell-shaped solitons, kink-type, singular and power series solution of CIMA chemical equations. In this thesis, we used sin-cosine method (SCM), $\csc h$ technique, $\tan - \cot$ method and RPSM architectonic. SCM retrieved bell-shaped, $\csc h$ approach provided singular solutions, $\tan - \cot$ technique gave kink solutions and RPSM provided power series solutions. We also obtained analytic and power series solution of ACFLV model. we used sub-ODE scheme (SOS) and RPSM architectonic. SOS retrieved bell type, kink type, anti-kink type solitons, JEF, WEF, hyperbolic function and parabolic function and RPSM provided power series solutions. To the best of our knowledge, our results are new and novel.

Chapter 5

References

[1] M. A. Ablowitz, P. A. Clarkson, Solitons, Nonlinear evolution equations and inverse scattering, *Cambridge University Press,* (1991) 532.

[2] N. N. Akhmediev, A. Ankiewicz, Solitons, non-linear pulses and beams, *Springer,* (1997).

[3] O. J. J. Algahtani, Comparing the AtanganaBaleanu and CaputoFabrizio derivative with fractional order: Allen Cahn model, *Chaos Solitons Fractals,* 89 (2016) 552559.

[4] H. M. Baskonus, T. A. Sulaiman, H. Bulut, On the novel wave behaviors to the coupled nonlinear Maccari's system with complex structure, *Optik,* 131 (2017) 1036-1043.

[5] C. Chen, Y. Jiang, Z. Wang, J. Wu, Dynamical behavior and exact solutions for time-fractional nonlinear Schrödinger equation with parabolic law nonlinearity, *Optik,* 222 (2020) 165331.

[6] S. T. Demiray, Y. Pandir, H. Bulut, New solitary wave solutions of Maccari system, *Ocean Engineering,* 103 (2015) 153-159.

[7] M. A. Dokuyucua, Caputo and Atangana-Baleanu-Caputo fractional derivative applied to Garden equation, *Turkish Journal of Science,* 5 (2020) 1-7.

[8] E. F. Donfack, J. P. Nguenang, L. Nana, Fractional analysis for nonlinear electrical transmission line and nonlinear Schrödinger equations with incomplete sub-equation, *The European Physical Journal Plus,* 133 (2018).

[9] P. G. Drazin, R. S. Johnson, Solitons: an introduction, *Cambridge University Press,* (1989) 226.

[10] S. Qureshi, A. Yusuf, A. A. Shaikh, M. Inc, D. Baleanu, Fractional modeling of blood ethanol concentration system with real data application, *Chaos: An Interdisciplinary Journal of Nonlinear Science,* 29(1), (2019) 013143.

[11] N. Raza, M. A. Ullah, A comparative study of heat transfer analysis of fractional Maxwell fluid by using Caputo and Caputo-Fabrizio derivatives, *Canadian Journal of Physics,* 98 (2020) 89-101.

[12] M. I. Syam, M. Al-Refai, Fractional differential equations with AtanganaBaleanu fractional derivative: Analysis and applications, *Chaos, Solitons & Fractals: X,* 2 (2019) 100013.

[13] M. Mirzazadeh, M. Ekici, A. Sonmezoglu, M. Eslami, Q. Zhou, A. H. Kara, D. Milovic, F. B. Majid, A. Biswas, M. Belic, Optical solitons with complex Ginzburg-Landau equation, *Nonlinear Dynamics,* 85 (3) (2016) 1979-2016.

[14] Wazwaz, A. M, Sine-cosine method for handling non-linear wave equations, *Math. Comput. Modelling,* 40 (2004) 499-508.

[15] Wazwaz, A. M, The Sine-cosine Method for obtaining solutions with compact and non-compact structures, *Appl. Math. Comput. Modelling,* 159 (2004) 559-576.

[16] M. Belic, M. Mirzazadeh, M. Eslami, E. Zerrad, M. F. Mahmood, A. Biswas, Optical solitons in nonlinear directional couplers by sine-cosine function method and Bernoullis equation approach, *Nonlinear Dyn.,* 81 (2015) 1933-1949.

[17] A. Biswas, H. Triki, Q. Zhou, S. P. Moshokoa, M. Z. Ullah, M. Belic, Cubic-quartic optical solitons in Kerr and power law media, *Optik,* 144 (2017) 357-362.

[18] A. Jaafar, M. Jawad, F. Jameel, I. A. Azzawia, A. Biswas, S. Khan, Q. Zhou, S. P. Moshokoad, M. R. Belic, Bright and singular optical solitons for KaupNewell equation with two fundamental integration norms, *Optik,* 182 (2019) 594-597.

[19] A. Ja'afar and M. Jawad, A reliable treatment of residual power series method for time-fractional BlackScholes European option pricing equations, *Applied Mathematics E-Notes,* 10 (2013) 103-111.

[20] V. P. Dubey, R. Kumar, D. Kumar, A reliable treatment of residual power series method for time-fractional BlackScholes European option pricing equations, *Physica A: Statistical Mechanics and its Applications,* 533 (2019) 122040.

[21] B. A. Mahmood, M. A. Yousif, L. Liu , A residual power series technique for solving Boussinesq-Burgers equations, *Cogent Mathematics,* 4 (2017) 1279398.

[22] B. Chen, L. Qin, F. Xu and J. Zu, Applications of general residual power series method to differential equations with variable coefficients, *Discrete Dynamics of Nonlinear Systems in Nature and Society,* 10 (2018) 2394735 .

[23] A. Arafa and G, Elmahdy, Application of residual power series method to fractional coupled physical equations arising in fluids flow, *Discrete Dynamics of Nonlinear Systems in Nature and Society,* 10 (2018) 7692849.

[24] B. Ghanbari and A. Atangana, A new application of fractional AtanganaBaleanu derivatives: Designing ABC-fractional masks in image processing. *Physica A*, 542 (2020) 123516.

[25] F. Jarada, T. Abdeljawad, Z. Hammouch, On a class of ordinary differential equations in the frame of AtanganaBaleanu fractional derivative. *Chaos, Solitons and Fractals*, 117 (2018) 16-20.

[26] K. M. Owolabi, Modelling and simulation of a dynamical system with the Atangana-Baleanu fractional derivative, *Eur. Phys. J. plus*, (2018) 133:15.

[27] O. J. Peter, A. S. Shaikh, M. O. Ibrahim, K. S. Nisar, D. Baleanu, I. Khan and A. I. Abioye1, Analysis and dynamics of fractional order mathematical model of COVID-19 in Nigeria using Atangana-Baleanu operator, *Tech Science Press*, 26 (2021) 02.

[28] S. T. R. Rizvi, A. R. Seadawy, I. Bibi, M. Younis, Chirped and chirp-free optical solitons for Heisenberg ferromagnetic spin chains model, *Modern Physics Letters B*, 35 (2021) 2150139.

[29] S. T. R. Rizvi, I. Ali, A. R. Seadawy, M. Younis, I. Bibi, Chirp-free optical dromions for the presence of higher order spatio-temporal dispersions and absence of self- phase modulation in birefringent fibers, *Modern Physics Letters B*, 34 (2020) 2050399.

[30] I. Lengyel and I.R. Epstein, Modeling of Turing structure in the Chlorite-iodide-malonic acid starch reaction system, *Science,* 251 (1991) 650-652.

[31] I. Lengyel, I. R. Epstein, A chemical approach to designing Turing patterns in reaction-diffusion system, *Proc. Natl. Acad. Sci,* 89 (1992) 3977-3979.

[32] A. Jaafar, M. Jawad, F. Jameel, I. A. Azzawia, A. Biswas, S. Khan, Q. Zhou, S. P. Moshokoad, M. R. Belic, Bright and singular optical solitons for KaupNewell equation with two fundamental integration norms, *Optik,* 182 (2019) 594-597.

[33] A. Ja'afar and M. Jawad, A reliable treatment of residual power series method for time-fractional BlackScholes European option pricing equations, *Applied Mathematics E-Notes,* 10 (2013) 103-111.

[34] M. M. A. Khater, M. S. Mohamed, H. Alotaibi, M.A. El-Shorbagy, S.H. Alfalqi, J. F. Alzaidi, D. Lu, Novel explicit breath wave and numerical solutions of an Atangana conformable fractional LotkaVolterra model, *Alexandria Engineering Journal,* 60 (2021) 47354743.

[35] E. M. E. Zayed, M. E. M. Alngar, A. Biswas, H. Triki, Y. Yldrm, A. S. Alshomrani, Chirped and chirp-free optical solitons in fiber bragg gratings with dispersive reflectivity having quadratic-cubic nonlinearity by sub-ODE approach, *Optik,* 203 (2020) 163993.

[36] M. Khalighi, L. Eftekhari, S. Hosseinpour, L. Lahti, Three-species Lotka-Volterra model with respect to Caputo and Caputo-Fabrizio fractional operators, *Symmetry,* 13 (2021) 368.

[37] A. Khaled, Gepreel, Extended trial equation method for nonlinear coupled Schrödinger Boussinesq partial differential equations, *Journal of the Egyptian Mathematical Society,* 85 (3) (2015).

[38] M. Ekici, M. Mirzazadeh, A. Sonmezoglu, M. Z. Ullah, Q. Zhou, H. Triki, S. P. Moshokoa, A. Biswas, Optical solitons with anti-cubic nonlinearity by extended trial equation method, *Optik,* 136 (2017) 368-373.

[39] A. J. M. Jawad, M. J. A. AlShaeer, Soliton solutions of the paraxial Schrödinger equations for Kerr law nonlinearity, *Hindawi*, (2018) 1-8.

[40] Alka, A. Goyal, R. Gupta, C. N. Kumar, Chirped femtosecond solitons and double-kink solitons in the cubic-quintic nonlinear Schrödinger's equation with self-steepening and self-frequency shift, *Physical Review,* 84 (2011) 063830.

[41] H. Triki, K. Porsezian, A. Choudhuri, P. T. Dinda, Chirped solitary pulses for a nonic nonlinear Schrödinger's equation on a continuous-wave background, *Physical Review,* 93 (2016) 063810.

[42] E. M. E. Zayeda, R. M. A. Shohiba, A. Biswas, Y. Yldrmf, F. Mallawic, M. R. Belic, Chirped and chirp-free solitons in optical fiber bragg gratings with dispersive reflectivity having parabolic law nonlinearity by Jacobis elliptic function, *Results in Physics,* 15 (2019) 102784

[43] E. M. E. Zayed, M. E. M. Alngar, A. Biswas, H. Triki, Y. Yldrm, A. S. Alshomrani, Chirped and chirp-free optical solitons in fiber bragg gratings with dispersive reflectivity having quadratic-cubic nonlinearity by sub-ODE approach, *Optik,* 203 (2020) 163993.

[44] S. T. R. Rizvi, A. R. Seadawy, S. O. Abbas, S. Latif, Saad Althobaiti, Exact and numerical solutions to the system of the chlorite iodide maloniic acid chemical reactions , *Computational and Applied Mathematics*, (2021) 41:13.